EUR 5147 e

Part 2 of 2

COMMISSION OF THE EUROPEAN COMMUNITIES

THE FIRST JOINT 900°C HTR FUEL IRRADIATION EXPERIMENT IN THE HFR PETTEN PROJECT E 96-01

POST-IRRADIATION EXAMINATION

1974

Joint Nuclear Research Centre
Petten Establishment - Netherlands

LEGAL NOTICE

This report is on sale at the addresses listed on cover page 4

at the price of B.Fr. 85.—

Commission of the
European Communities
D.G. XIII - C.I.D.
29, rue Aldringen
L u x e m b o u r g

August 1974

EUR 5147 e
Part 2 of 2

COMMIS[illegible] OF THE EUROPEAN COMMUNITIES

THE FIRST J[illegible]NT 900°C HTR FUEL IRRADIATION EXPE[illegible]ENT IN THE HFR PETTEN

P[illegible]

A[illegible]

G. DA[illegible]
H. JA[illegible]
Th. SCHOOT

EUR 5147 e
Part 2 of 2

THE FIRST JOINT 900 °C HTR FUEL IRRADIATION EXPERIMENT IN THE HFR PETTEN
PROJECT E 96-01
Post-Irradiation Examination

Commission of the European Communities
Joint Nuclear Research Centre - Petten Establishment (Netherlands)
Luxembourg, August 1974 - 68 Pages - 48 Figures - B.Fr. 85.—

The ,,900 °C irradiation experiment'' has been executed in the HFR reactor at Petten to investigate the performance of a large variety of HTR fuel over a range of burn-up and fast neutron doses with fuel surface temperatures of about 900 °C.

The results of post-irradiation examination are presented together with some remarks and suggestions in order to improve the fuel performance and the production costs.

EUR 5147 e
Part 2 of 2

THE FIRST JOINT 900 °C HTR FUEL IRRADIATION EXPERIMENT IN THE HFR PETTEN
PROJECT E 96-01
Post-Irradiation Examination

Commission of the European Communities
Joint Nuclear Research Centre - Petten Establishment (Netherlands)
Luxembourg, August 1974 - 68 Pages - 48 Figures - B.Fr. 85.—

The ,,900 °C irradiation experiment'' has been executed in the HFR reactor at Petten to investigate the performance of a large variety of HTR fuel over a range of burn-up and fast neutron doses with fuel surface temperatures of about 900 °C.

The results of post-irradiation examination are presented together with some remarks and suggestions in order to improve the fuel performance and the production costs.

Joint Nuclear Research Centre
Petten Establishment - Netherlands

ABSTRACT

The ,,900 °C irradiation experiment'' has been executed in the HFR reactor at Petten to investigate the performance of a large variety of HTR fuel over a range of burn-up and fast neutron doses with fuel surface temperatures of about 900 °C.

The results of post-irradiation examination are presented together with some remarks and suggestions in order to improve the fuel performance and the production costs.

CONTENTS

1. INTRODUCTION

A large variety of coated particles has been irradiated as monolayer and small size compacts.All the varieties of irradiated particles were coated by triplex layers:PyC-SiC-PyC.
The particles were prepared in three different laboratories with the geometry of the coating as a variable.
The fuel in the kernel was present as UO_2 and $(Th,U)O_2$ spheres with nominal diameters of 650 and 800 μm.The UO_2 spheres were manufactured by a slow growth agglomeration process and the $(Th,U)O_2$ by emulsion.
The original aim of this experiment was to irradiate standard HTR coated particles at 900°C to a final fast neutron dose of about $4x10^{21}$ n/cm^2 N.D.E. with a burn-up,depending on the enrichment,between 5 and 12% fima (1).
As consequence of failure of the irradiation rig the experiment was stopped at the moment the contents had received a fast neutron dose of 1.1×10^{21} n/cm^2 N.D.E.
The dismantling operation has been started about six months after the rig was removed from the reactor core because,at the very beginning the intention was to replace the failed rig and to continue the irradiation.
The post-irradiation examination has been carried out at Petten by EURATOM and R.C.N. jointly.

2. GAMMA-SCANNING AND AUTORADIOGRAPHIC EXAMINATIONS

Before starting the dismantling of the primary stainless-steel container where the fuel was located,a preliminary longitudinal gamma-scan was performed.In fig.1 and 2 are presented the profile

of the levels of activity of Co-60 and Mn-54 respectively.
A scanning step of 1 cm was used.A second longitudinal gamma-scan of the assembled fuel including the graphite box containers was realised by steps of 2 mm and was devoted to the examination of the level of activity of selected fission products.
In fig.3,4,5,6,and 7 are presented the distribution of the levels of activity,in arbitrary units,of Ce-141,Ce-144,Ru-/Rh-106 Zr-95 and Cs-137.
Once the monolayers and the small size compacts had been removed from the graphite boxes,the possibility of realising a gamma-scan of the empty boxes was checked,but the level of activity was too low in comparison to the back-ground of the cell.
However some information on the contamination level of the internal wall of the graphite boxes was obtained by autoradiographic technique.In fig.8,9 and 10 are presented the autoradiographic images of some of the boxes together with the corresponding profile of Zr-95 distribution already presented in fig. 6. As can be observed there is a strict correspondence between the level of fission product present in the fuel and the degree of wall contamination,with the one exception in correspondence of the peak of activity due to compacts with 0.4 % of enrichment,where the autoradiography shows a region of low contamination. One explanation of the observed divergence could be that the blackening of the film is essentially generated by the activity of a radio-isotope for which the fission product yield is largely different in the fission of U-235 and of U-238.
During the unloading of the graphite boxes an optical inspection of the monolayers and compacts was executed.No modification of the surface condition was observed.In fig.11 is presented

a view of the fueled bodies.

3. DIMENSIONAL MEASUREMENTS

Dimensional measurements were executed before and after irradiation.As a consequence of the very small tendency in contraction of the samples observed in post-irradiation examination,the dimensional measurements were restricted to the variation of the external diameter of monolayers and compacts. The measured values are presented in the tables labelled from I to XII .

4. MICRO-RADIOGRAPHIC EXAMINATIONS

Radiographs were taken of each monolayer before and after irradiation with a special X-ray device (2) .

Comparing the images of each monolayer it is possible to observe the presence of phenomena generated or enhanced by the effects of irradiation and temperature.

The correspondent radiographic images of a few particles taken before and after irradiation are presented in fig.12,13,14,15, 16 and 17 in order to give a general idea of the observed phenomena.

Examining the micro-radiographs,under microscope,it is possible to observe each component present in the monolayer,as is evident in fig. 17b. Generally the magnified images presented in the paper show the SiC layer and what is inside it. This is the consequence of the choosen intensity of light and of the choosen exposure time in order to reveal,with the best contrast,the region surrounding the kernel.

Some of the phenomena observed in post-irradiation examinations were present in a few monolayers before the irradiation,but in a less pronounced way. This means that some of the observed phemomena is not strictly a result of irradiation but of something in the manufacturing or consolidation process of the compacts.

On the other hand we have observed in the unirradiated state the evolution of the kernel contraction phenomenon and the subsequent kernel penetration into the coating under the effect of isothermal heat treatment (3) .

As far as the UO_2 kernel is concerned the predominant phenomenon is contraction of the kernel as is shown in fig.15b, which can be ascribed to a sintering process.

Generally,the kernel during the volume contraction phenomenon remains bonded with about 1/3 of its surface to the pyrocarbon coating, this will generate an eccentricity of the kernel in the particle.

When kernel contraction takesplace,it is generally possible in the radiograph to observe the original kernel position or profile,as a track due to the presence of heavy metals in the coating. The region is delimited by the original and the new kernel profiles; without heavy metal contamination as appears in fig. 15b and 18a or with a distribution of spots due to heavy metal contamination as appears in fig. 18d and 19.

Sometimes the original kernel profile is not very well visible,as can be seen in fig. 13b,and the evacuated region appears completely clean.

Some particles of a same batch embedded in the same monolayer show different stages of evolution of the kernel contraction phenomenon;others show no contraction at all, and yet others,on the contrary,show the kernel spreading to fill the buffer and seal layer regions. Fig.18 presents four particles located in the same monolayer and showing different kernel behaviour;fig. 20 shows a particle with

spreading of the kernel.

A parameter that can control the sintering or kernel contraction phenomenon is certainly the temperature,but it is not the only one. As a matter of fact,the heat treatment of an unirradiated monolayer compact,under isothermal condition has shown particles with their coatings destroyed by kernel penetration,particles with more or less kernel contraction phenomenon and particles unaffected by the phenomenon. This means that some other parameter in addition to the temperature can influence the evolution of the phenomenon;for instance coating integrity and presence of uranium carbide.

Some orientative evaluation of the volume contraction was performed utilizing a planimeter in order to determine the mean radius of the kernel in the radiographic images,before and after the irradiation. V_o represents the kernel volume of each particle before the irradiation.In table XIII are reported the $\Delta V/V_o$ values related to a variety of particles present in a monolayer and for which the nominal porosity of the kernel was of 17,3 %. In the considered monolayer were present 29 particles,16 of them showing contraction of the kernel. As far as $(Th,U)O_2$ kernels are concerned,very little sintering phenomenon is to be expected taking into consideration that the nominal density is nearly theoretical.In fact, sometimes it is possible to observe some small local kernel contraction as in fig.21. The arrows indicate the presence of cracks through the coating.

Similar cracks are also present in the UO_2 particles as can be seen in fig. 12,14b,15,16b,17b,18b and 22.

The identification of the cracks was made by examining the

radiographs under the microscope. The presented pictures do not show the cracks as clearly as they appear under the microscope.

As far as coatings are concerned, in addition to the already mentioned cracks that generally do not penetrate the outer pyrocarbon layer, it is possible to observe phenomena which are interpreted as lack of adherence at the buffer-seal layer interface or at the seal-inner pyrocarbon interface or to both the interfaces as consequence of the pyrocarbon shrinkage. Some of these phenomena are presented in fig. 12b, 20, 23, 24, 25 and 26.

Exceptionally, some batches present the SiC layer before and after irradiation with an apparent contamination of heavy metal as shown in fig. 27. A possible interpretation of the phenomenon is that during the deposition of the SiC layer in the fluidized bed, broken particles were present resulting in a high uranium contamination and local reactions. No visible change has been introduced by the irradiation.

5. Ceramographic examinations

Ceramographic examinations performed on a few selected samples have confirmed the presence of the phenomena already observed during the analysis of the radiographs. Particularly in the ceramographic views there is evidence of phenomena like kernel contraction, cleavage at the buffer-seal layer interface or at the seal-inner pyrocarbon interface, and cracks in the inner pyrocarbon layer and buffer. Particularly interesting is the effect of the

irradiation on the buffer layer of some varieties of particles as is shown in fig. 28, 29 and 30.

The figures 31, 32 and 35 are pertinent to particles, the kernel of which was of the $(Th,U)O_2$ type. This type of kernel as consequence of the nominal density being close to the theoretical one, has not presented any sintering phenomenon during the irradiation, hence the observed gap between buffer and inner pyrocarbon layer must be interpreted as being due to densification and shrinkage of the pyrocarbon material.
The other figures showing cleavage effect at the interface of the buffer and seal layers show also deformation and breakage of the buffer layer as is evident in the figures 29 and 30.
In fig. 33 can be observed one variety of particles showing the presence of porosity in the silicon carbide shell.
Some other ceramographic views are presented in the figures 34, 36, 37, 38 and 39.

The agreement between radiographic and ceramographic examination offers the opportunity of reducing the ceramographic preparation to those samples of particular experimental interest, selected on the basis of the radiographic examination.

6. Solid fission products and free uranium present in the monolayer matrix.

From a few monolayer compacts the particles were separated from the matrix utilizing a mixture of sulfuric and nitric acid. After a few minutes a complete desintegration of the coupons was achieved. To dissolve also the outer pyrocarbon layer, prolonged action was necessary.
After the separation the matrix material has been completely dissolved. The recovered particles were washed in 25 ml 0.1 N nitric acid and then boiled for two hours in 25 ml 6 N nitric acid.
From the solution containing the dissolved matrix and from the second nitric acid solution, samples were taken. Those samples were counted in a fixed geometry. The spectra, fig. 40, 41, 42, 43, 44 and 45, are comparable with each other, they differ only in counting time. Among the analyzed samples, the lowest amount of solid fission products was observed in the sample D and the highest in the sample C.
Another interesting parameter was the amount of free uranium present in the matrix and in the leaching solution. The method we applied was based on the U-238 (n,γ) U-239 reaction in the epithermal neutron region.
Aliquots of the solution were irradiated in cadmium capsules. The 75 keV γ-ray of U-239 was measured. After correction for decay the following results were obtained.

Monolayer	µg U(matrix)	µg U(leach)
A (6A-4)	< 15	< 0.5
B (122)	31	< 1
C (94)	280	14
D (82)	< 16	< 0.5
E (K62)	< 140	< 9
F (K63)	< 140	< 4

A worthful comparison may be a comparison with the uranium present in the matrix of unirradiated samples from the same batches.
The corresponding values are

batch type	µg U(matrix)
A	8
B	3
C & D	3
E & F	35

The presented values do not pretend to give the merit of the examinated samples on account of their low statistical value, but qualitatively they show the presence of cracks in the coatings of some varieties.

7. Absolute activity determination of Ce-144, Ru-106 and Cs-137 and burn-up determination.

Among the irradiated monolayers three were chosen for the absolute activity determination of some solid fission products. The selected samples are 3-G-3 (Dragon), K45 (KFA) and 12 (BN).
The matrix and the particles were desintegrated with the help of a mixture of sulfuric acid and nitric acid. After desintegration particles and matrix were separated.
The matrix was dissolved in a mixture of sulfuric acid and sodiumpersulfate. The particles were fused with sodiumhydroxide and sodiumperoxide (1:2). The melt was dissolved in nitric acid-hydrogenperoxide. Both solutions were diluted till known volumes. Aliquots were taken for analysis.

In the soulution with the dissolved particles as well as uranium as the absolute activities of Ru-106, Cs-137 and Ce-144 were determined. In the matrix solution we determined only the activities. To obtain the uranium content two techniques were applied. A spectrophotometric one based on a separation of the uranium by means of an ion-exchange technique and colouration with the help of oxine. The other technique was the activation method as described. The absolute activities were determined by comparing the activity measurements with measurements of standards obtained from the Radiochemical centre in Amersham.

Dragon coupon 3 G 3

From this coupon was known the enrichment of 3% and the amount of uranium in the coupon about 40 mg. The spectrophotometric measurements delivered the values 34.0 and 34.1 mg. Activation analysis, after correction for enrichment, 34.0 - 34.4 - 33.3 - 33.7 - 33.7 mg. Mean 33.9 $\pm$ 0.4 mg.

The absolute activities were (on 1-5-1973):

	matrix (µCi)	particles (mCi)
Cs^{137}	0.63	2.26
Ce^{144}	4.7	15
Ru^{106}	55	1.1

From the absolute activities the number of fissions were calculated using the following numbers:
Cs-137 fission yield 6.26%, half-life 30.0 y
Ru-106 " " 0.39%, " " 368 d
Ce-144 " " 5.44%, " " 284 d.

For the three isotopes a correction had to be made for decay during and after irradiation, until 1-5-1973. Those factors were Cs-137, 1.038; Ru-106 3.19 and Ce-144 4.49.
The number of fissions calculated from those isotopes are Cs-137 $1.89.10^{18}$, Ru-106 $1.53.10^{18}$ and Ce-144 $1.62.10^{18}$.
For the burn-up the results from the cesiumisotope was used, which resulted in 2.2% FIMA for this Dragon sample.

Belgo-nucleaire 12

This coupon contained 8.58% enriched uranium probably 14.8 mg. The spectrophotometric method delivered two results 12.4 and 12.2 mg, activation analysis, after correction for enrichment, 12.5 - 12.6 -12.4 -12.7 - 12.9, mean 12.5 $\pm$ 0.2 mg uranium.
The absolute activities were (on 1-5-1973)

	matrix (μCi)	particles (mCi)
Cs-137	0.62	1.54
Ce-144	1.1	11.7
Ru-106	1.4	0.10

The number of fissions are Cs-137 $1.29.10^{18}$, Ru-106 $1.39.10^{17}$ (?) and Ce-144 $1.27.10^{18}$.
From the cesium results a burn-up value of 3.9% FIMA was calculated.

KFA-45

This coupon contained 1.351 mg 89.42% enriched uranium while the thorium/uranium-235 ratio was 6.22.
A direct determination of uranium was not possible probably caused by a contamination of unirradiated uranium.

The absolute activities were (on 1-5-1973)

	matrix (μCi)	particles (mCi)
Cs-137	1.3	1.33
Ce-144	7.4	7.7
Ru-106	1.3	0.84

The number of fissions are Cs-137 $1.11.10^{18}$, Ru-106 $1.17.10^{18}$ and Ce-144 $0.83.10^{18}$.
From the cesium result a burn-up value of 4.7% FIMA was calculated.

8. General considerations

On the basis of the experimental observations in the post irradiation examination, and taking into consideration the experimental results coming out from experiments carried out on unirradiated materials, we are driven to believe that a large number of cracks can be introduced in the different coating layers as a consequence of the thermal history of the deposition process.
The time of life of coated particles under operative conditions can be considerably reduced as a consequence of coating damage caused during the manufacture or during the consolidation of particles in compact.
The generation of cracks in the buffer layer at the moment the deposition temperature will be increased in order to make the subsequent coating layer, will introduce in the UO_2 kernel the presence of uranium carbide as consequence of the CO release. The presence of uranium carbide in a UO_2 kernel of low density seems to have an accelerating effect on the sintering process of the kernel. Such a sintering leaves the kernel in an eccentric position and bonded to the buffer layer by only a small region of the surface. This means that the coating during irradiation will be under unisotropic conditions as regard to the temperature distribution and the radiation damage by fission fragments. In fig. 46 are presented radiographic images of pieces of coating collected during a crushing test on unirradiated particles. It is possible to observe the crack networks that were present in the buffer and

seal layers. The networks are heavy metal tracks on the inner face of the inner pyrocarbon layer.

In fig. 47 is presented the radiographic images of an unirradiated particle after a crushing test. It is possible to observe the original kernel profile and the large kernel contraction, but at the same time in the fragment of coating it is also possible to observe the crack network. The generation of cracks in the silicon layer at the moment the deposition temperature will be increased, in order to make the subsequent coating layer, or at the moment of particle consolidation in compact, as mechanical stress, or at the moment of graphitization of matrix as temperature effect, will considerably reduce the fission barrier power and the life of the whole coating. When the cracks in the SiC layer are generated at the moment the outer pyrocarbon layer will be deposited the cracks can be spread from SiC over the inner pyrocarbon layer.

It is our opinion that attention must be payed in order to make coatings under isothermal conditions instead of a sequence of temperature steps, and that the choosen deposition temperature must never be overtaken in the fuel consolidation operation and during reactor operation.

As far as the presence of uranium carbide in a UO_2 kernel and its behaviour is concerned, it is our opinion that some supplementary investigation must be planned in order to investigate its effect on the sintering process, on the capability

of retention of fission products in the kernel and on the reduction of the partial pressure of CO.

Particularly, experiments must be carried out on UO_2 kernels of low and high density containing tracks of uranium carbide surrounded by intact coatings. A better understanding of the observed phenomena could lead to a further improvement in the behaviour of the particles under irradiation and might permit reactor operation at higher temperatures with a further reduction of production costs.

No damage of the matrix has been observed either in monolayers or in small size compacts.

References

(1) The first joint 900°C HTR fuel irradiation experiment in the HFR PETTEN. Project E 96-01.

Part 1 of this EUR-report: Irradiation history, H. Röttger.

(2) In cell contact-microradiography, A. Drago - W. Huber. EUR 5015e.

(3) Experimental observation of UO_2 kernel/PyC coating interaction, A. Drago. EUR.

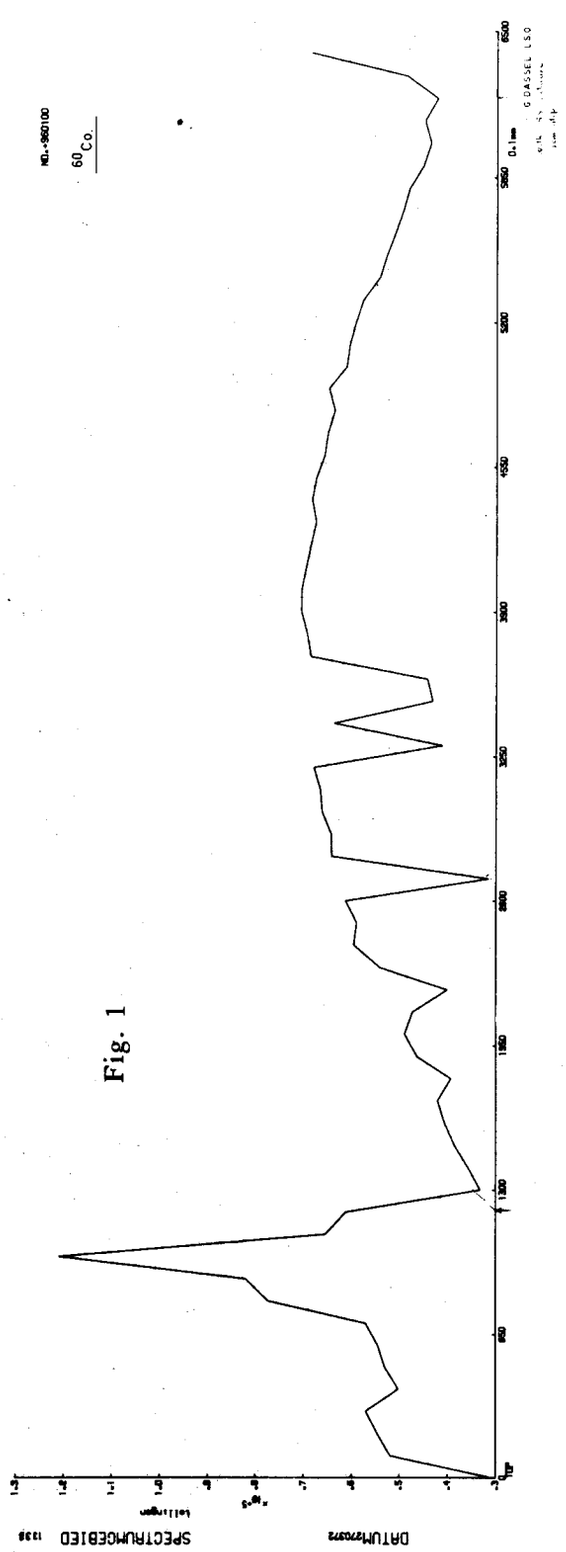
MD.-960100
60Co.
DATUM7x0372
SPECTRUMGEBIED

Fig. 1

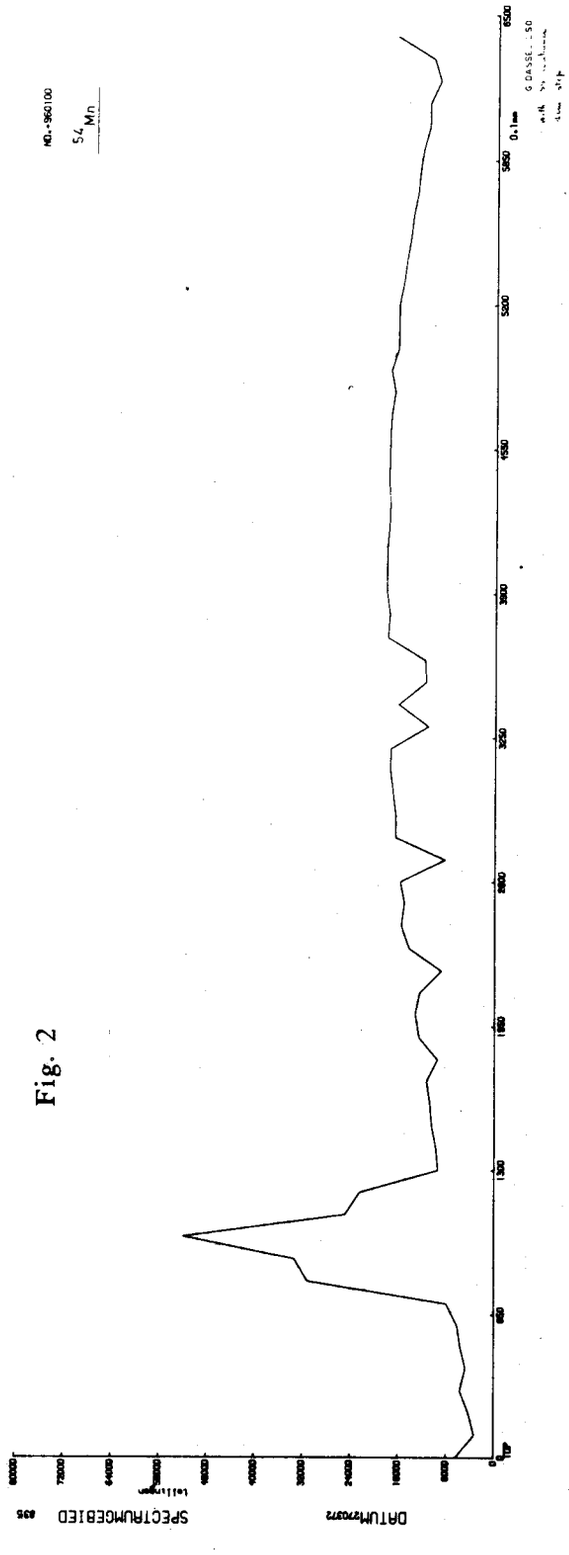
MD.-960100
54Mn
DATUM7x0372
SPECTRUMGEBIED

Fig. 2

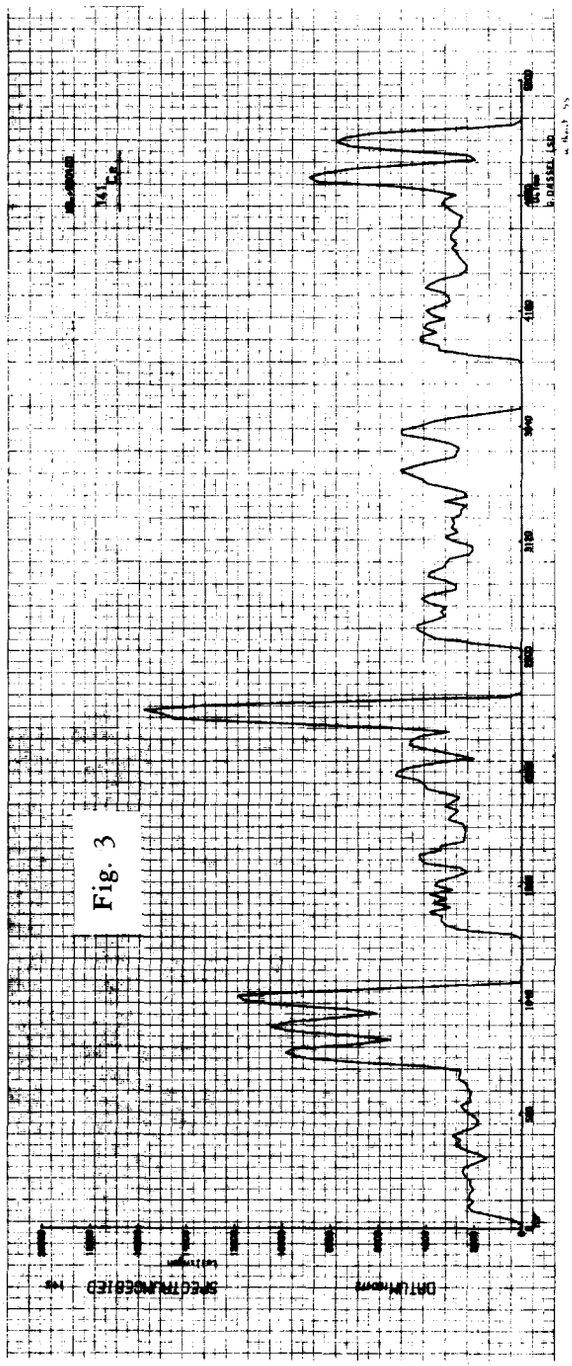

Fig. 3

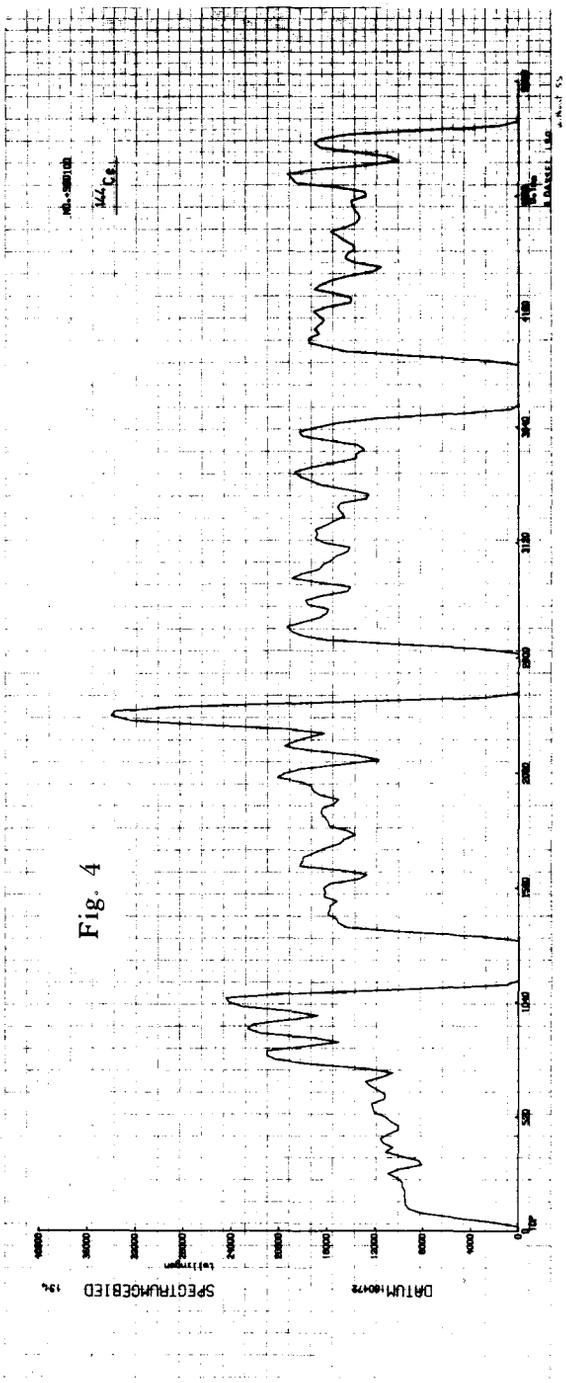

Fig. 4

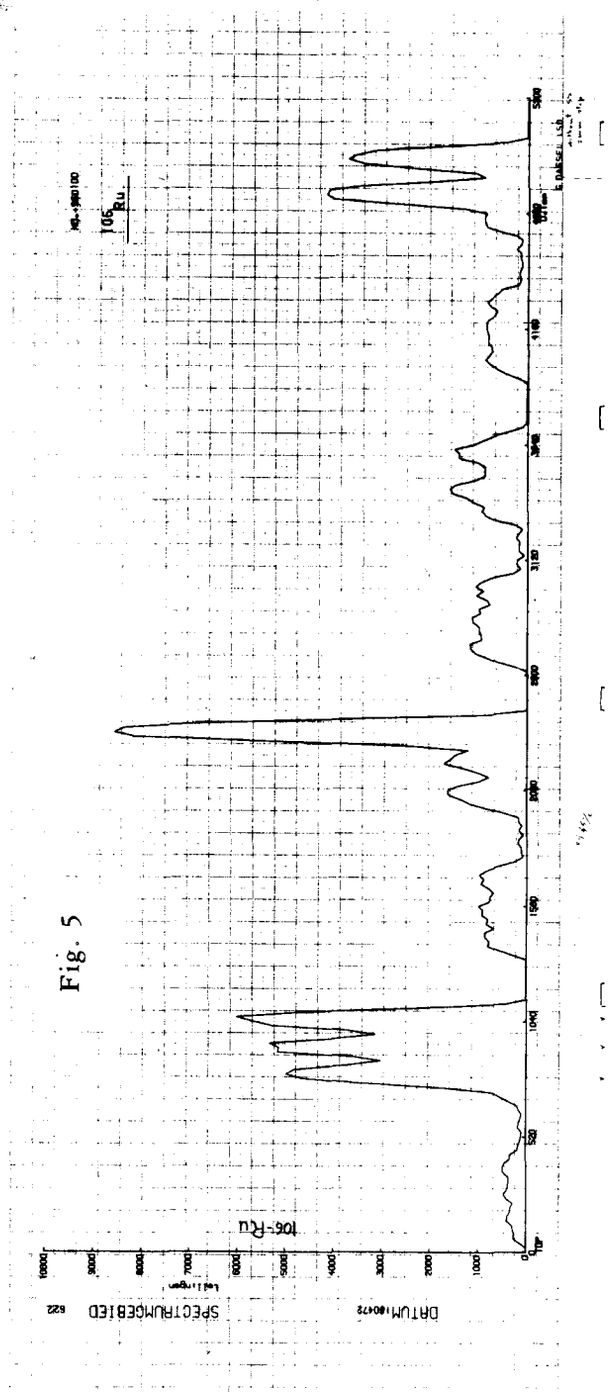
106 Ru
DATUM 160472
SPECTRUMGEBIET
106-Ru

Fig. 5

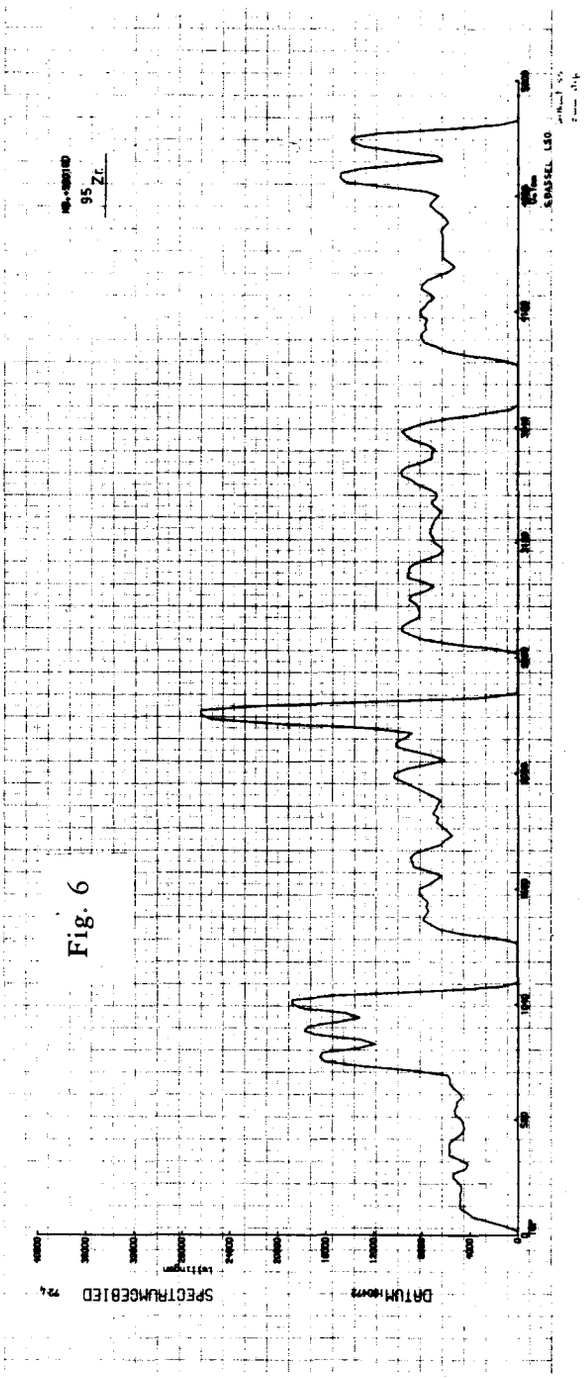
95 Zr
DATUM 160472
SPEKTRUMGEBIET

Fig. 6

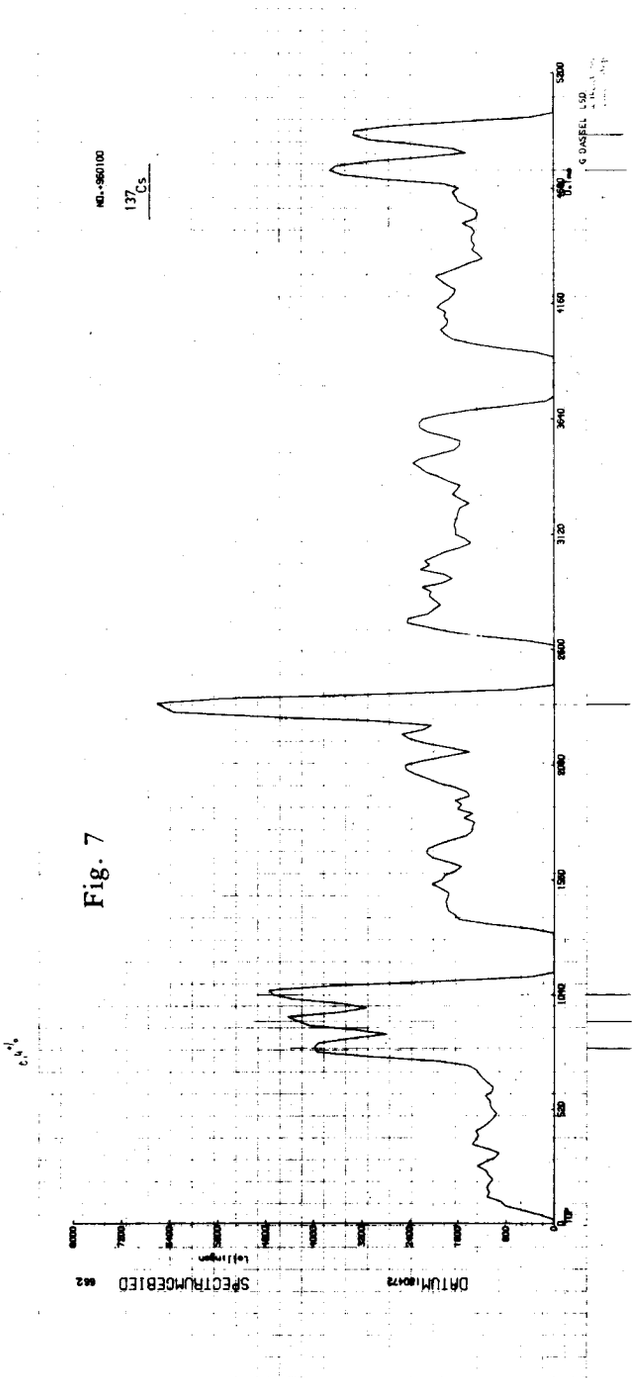

Fig. 7

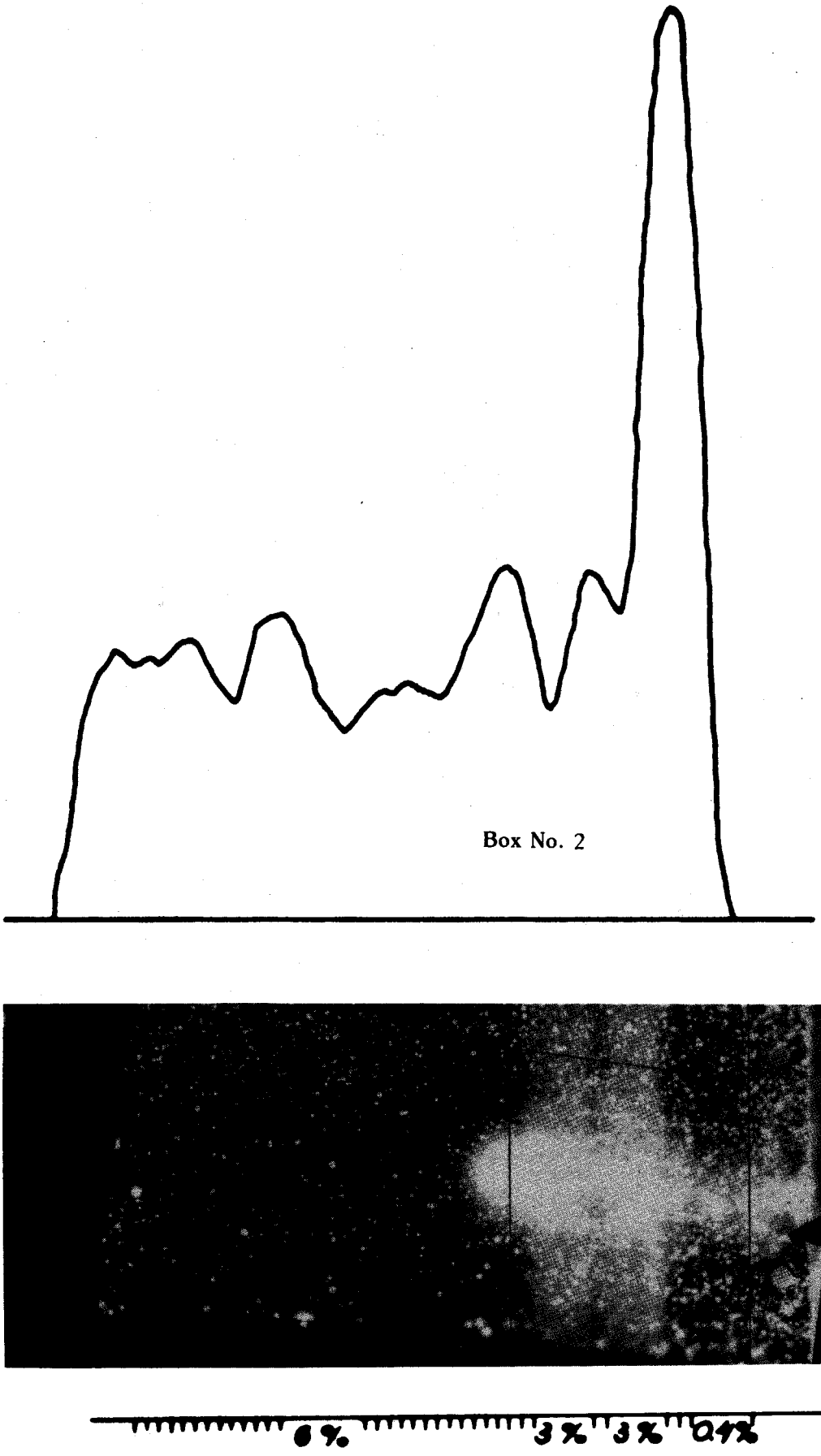

Fig. 8 Profile of the Zr^{95} distribution in the samples contained in the box n° 2, autoradiography of the inner-wall of the graphite box and samples arrangement in the box.

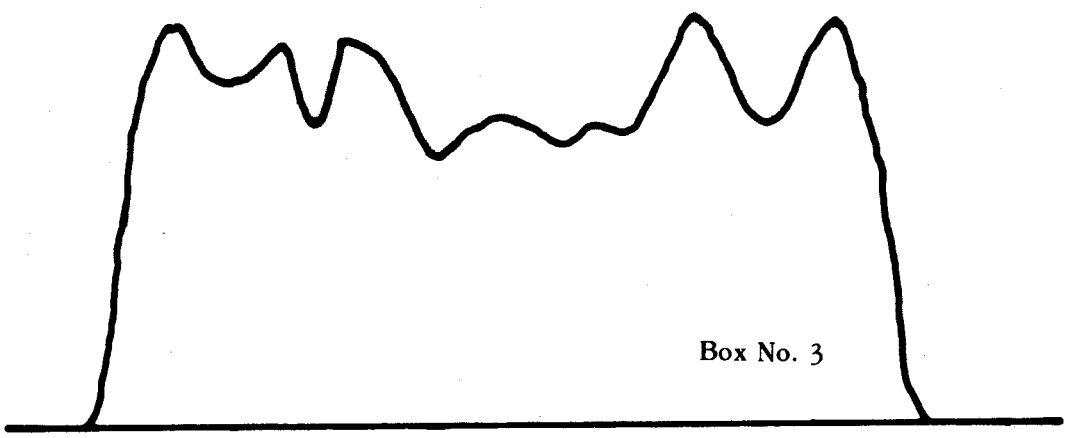

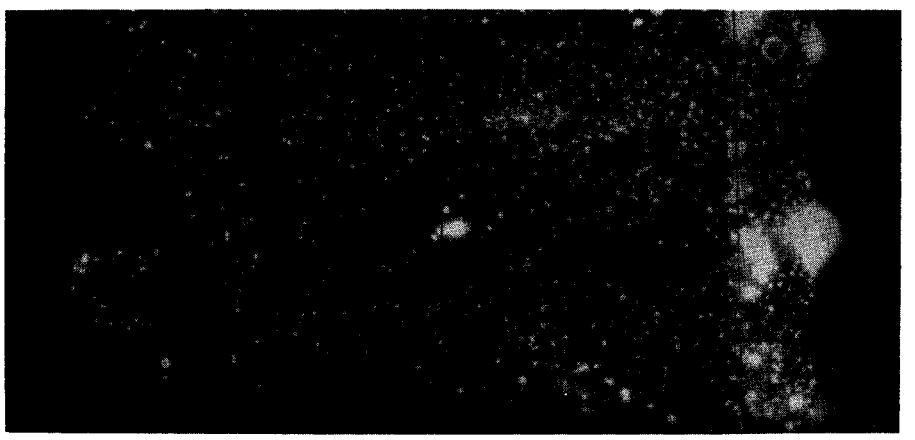

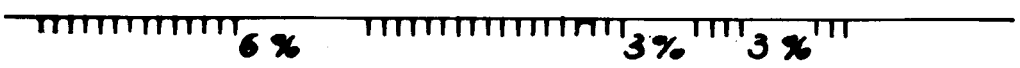

Fig. 9 Profile of the Zr^{95} distribution in the samples contained in the box n° 3, autoradiography of the inner-wall of the graphite box and samples arrangement in the box.

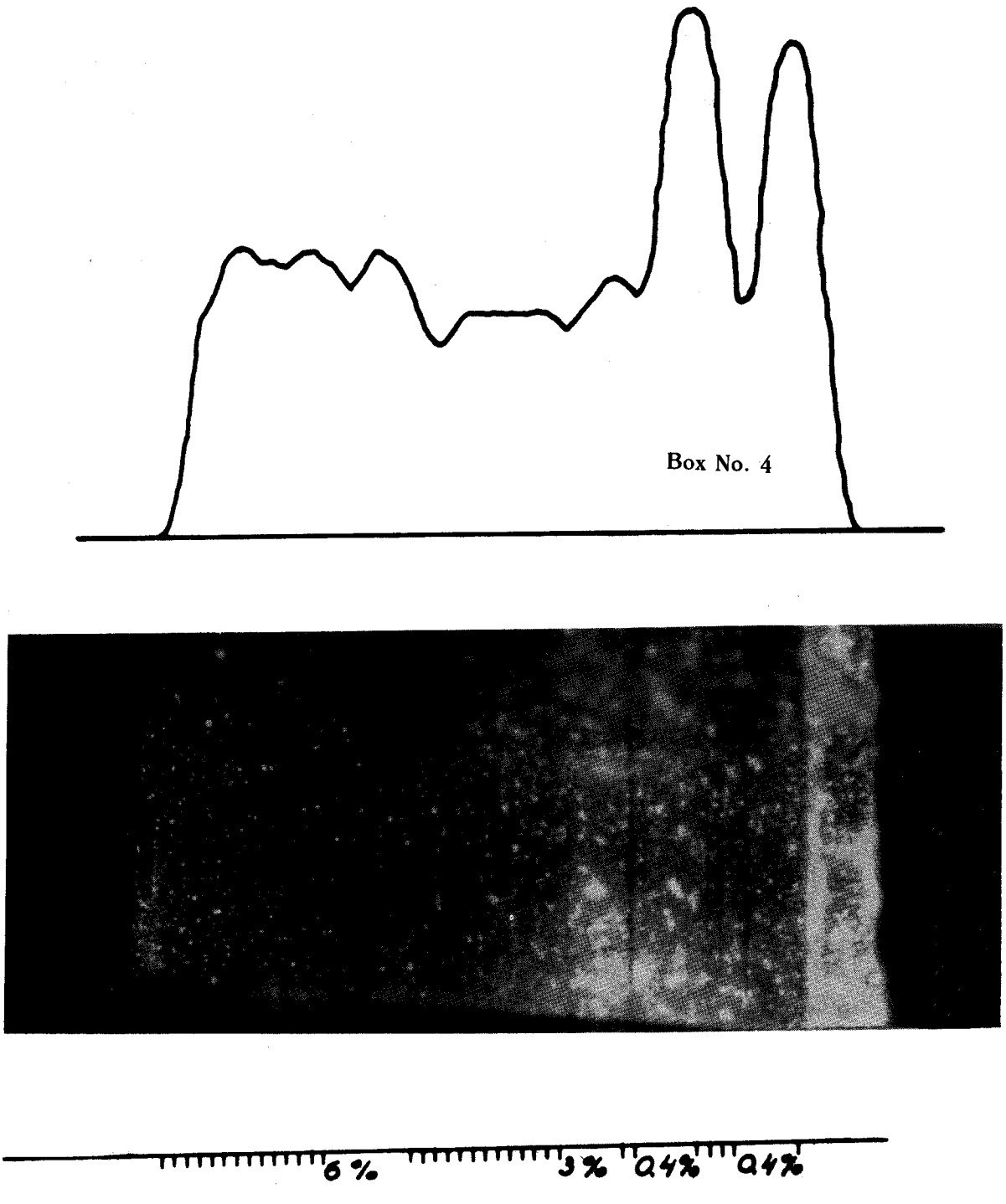

Fig. 10 Profile of the Zr^{95} distribution in the samples contained in the box n° 4, autoradiography of the inner-wall of the graphite box and samples arrangement in the box.

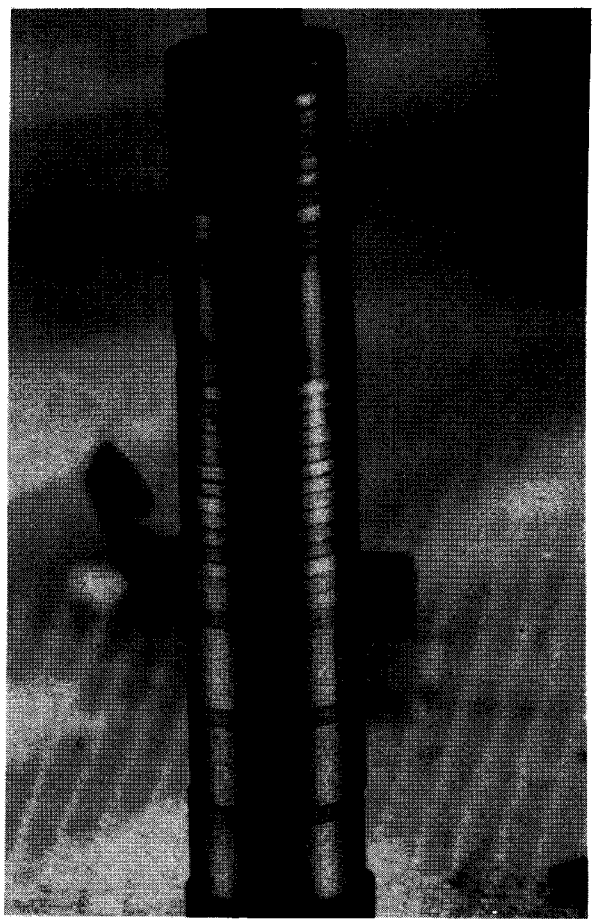

Fig. 11 View of the assembled monolayers and compact of a box after irradiation.

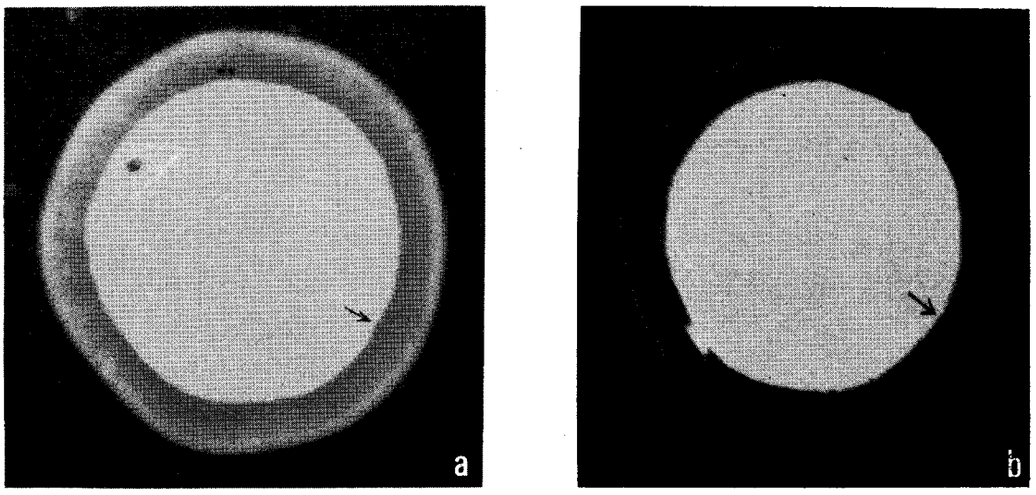

Fig. 12 Radiography of the same particle taken before (a) and after (b) the irradiation (monolayer 3E–3).

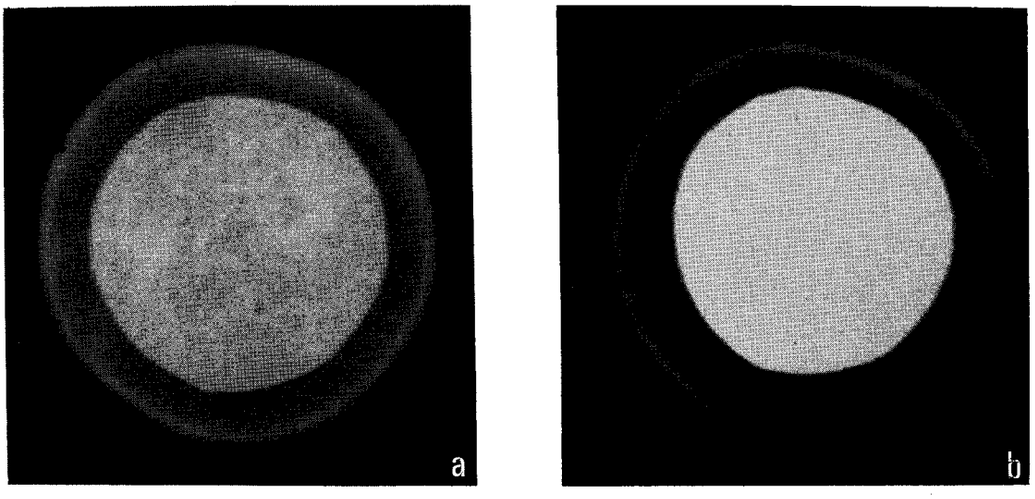

Fig. 13 Radiography of the same particle taken before (a) and after (b) the irradiation (monolayer 3E–3).

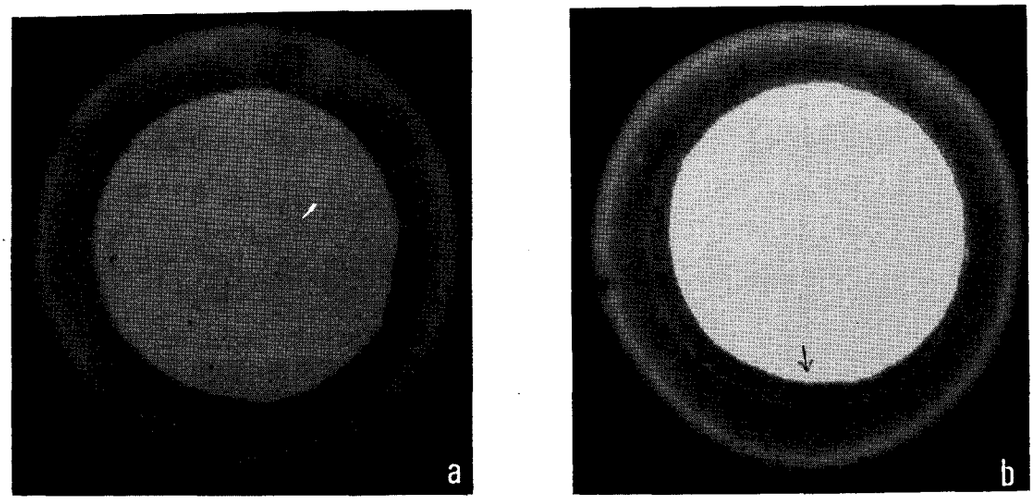

Fig. 14 Radiography of the same particle taken before (a) and after (b) the irradiation (monolayer 6G–3).

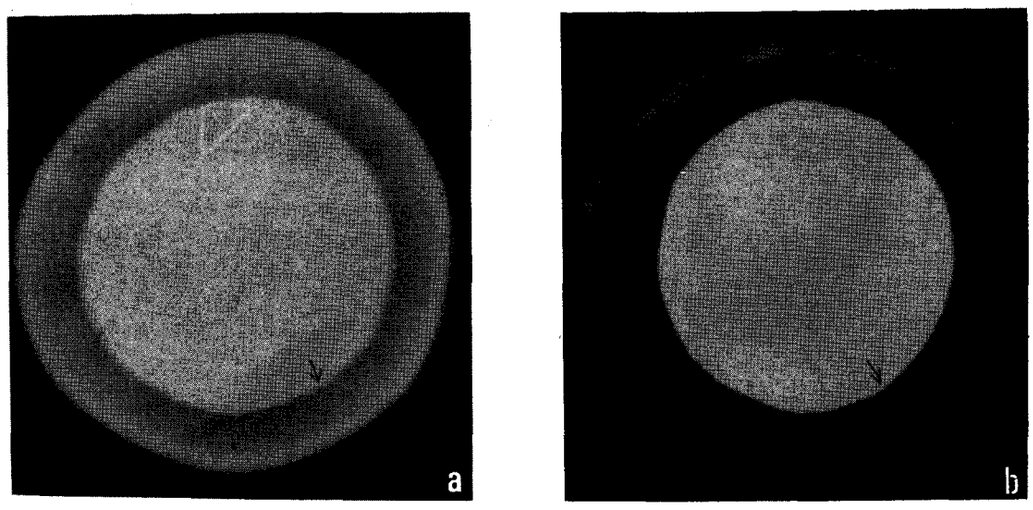

Fig. 15 Radiography of the same particle taken before (a) and after the irradiation (monolayer 6G–3)

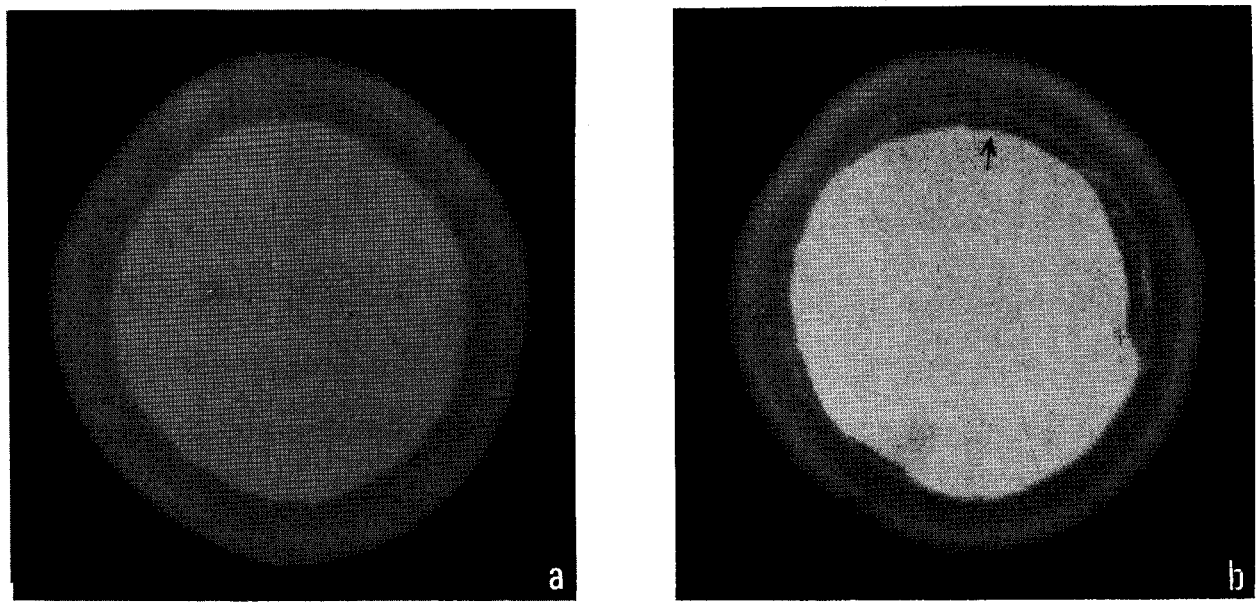

Fig. 16 Radiography of the same particle taken before (a) and after (b) the irradiation (monolayer 3L–3)

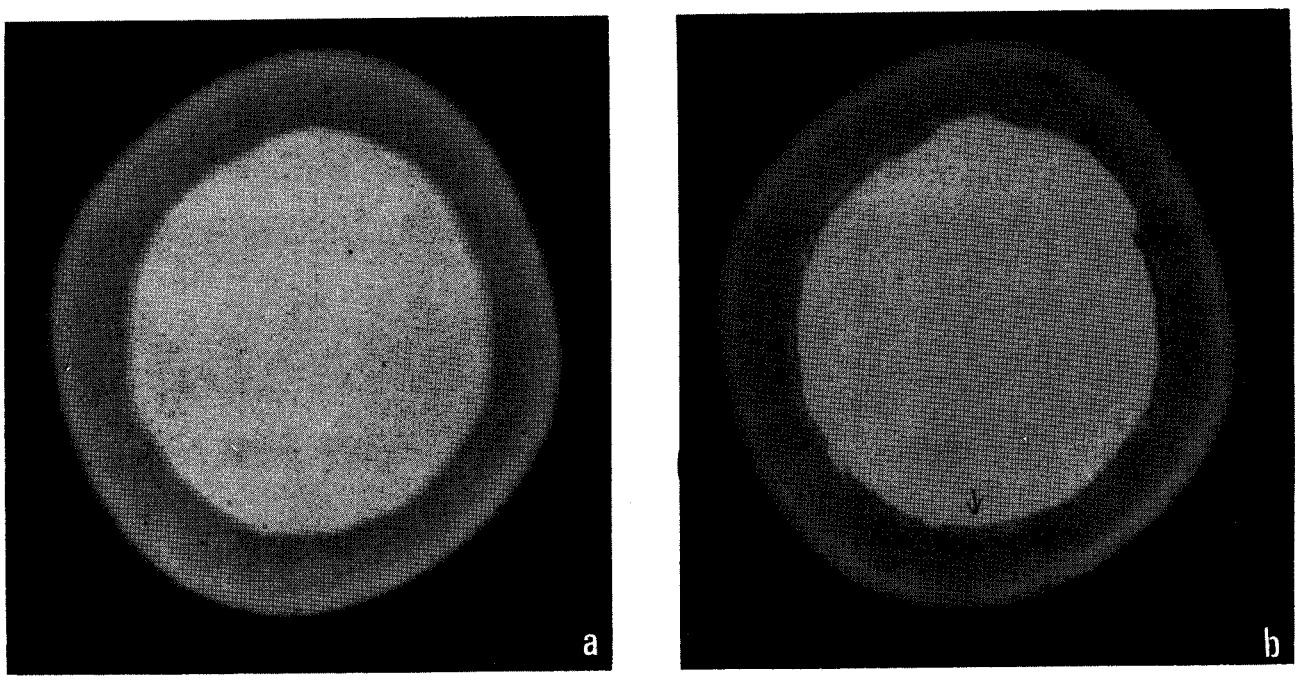

Fig. 17 Radiography of the same particle taken before (a) and after (b) the irradiation (monolayer C3–74).

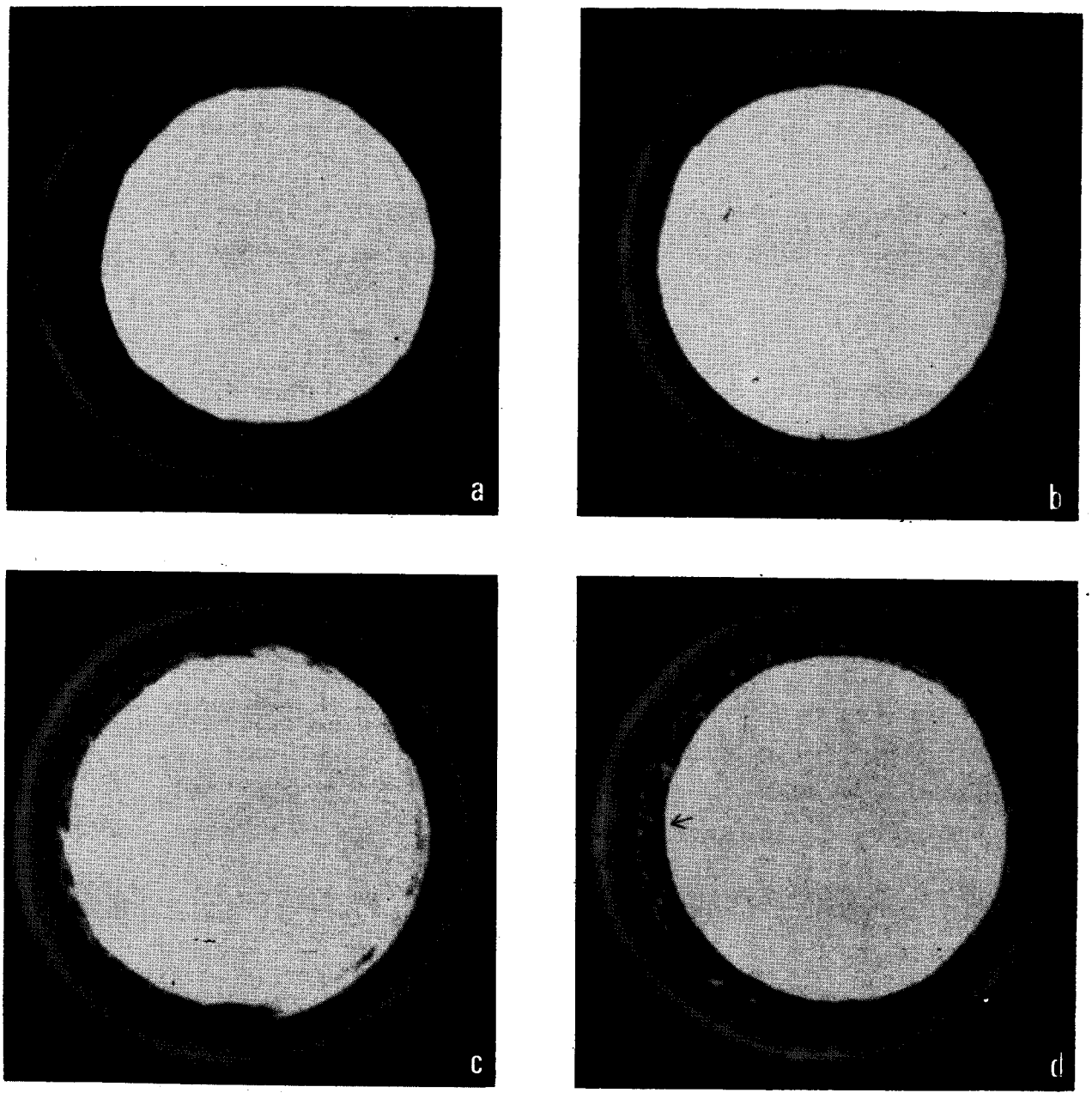

Fig. 18 Radiography of four particle present in the same monolayer taken after the irradiation (monolayer 3A–3).

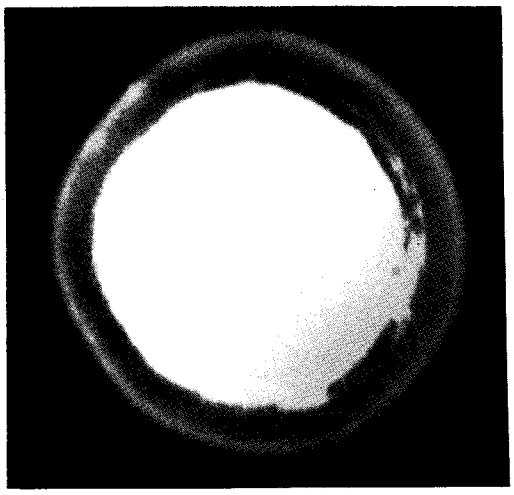

(monolayer 3E–5)

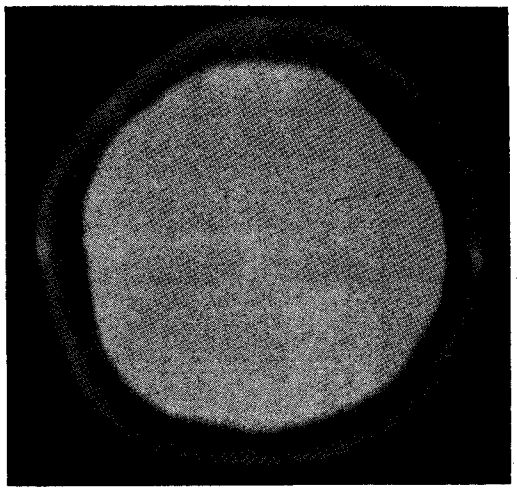

(monolayer 3E–5)

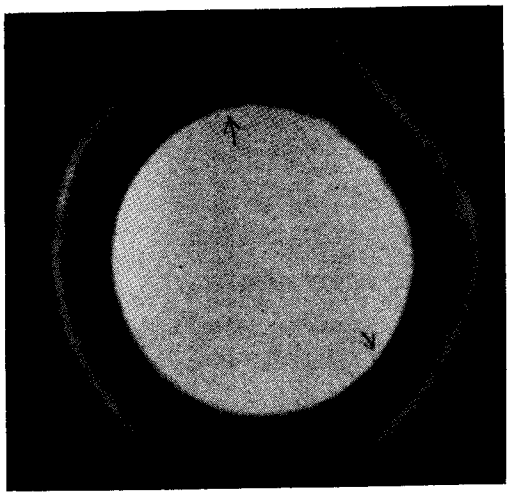

(monolayer K–41)

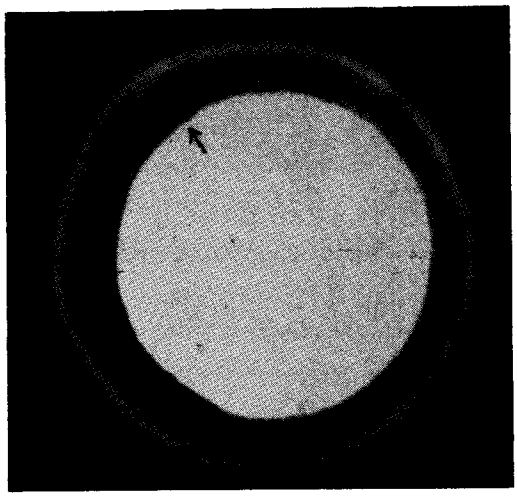

(monolayer 12E–3)

Fig. 19–22 Post-irradiation radiography of particles

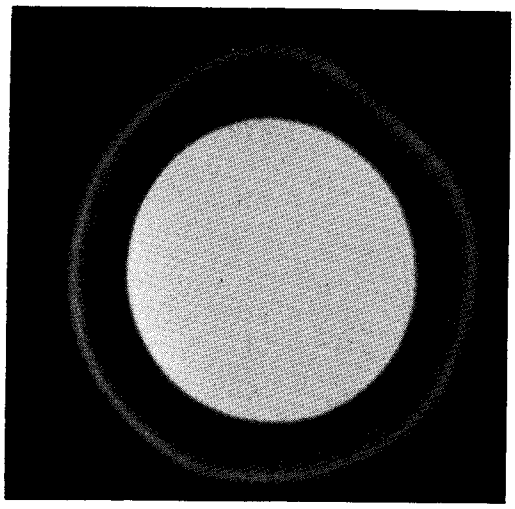

(monolayer K–41)

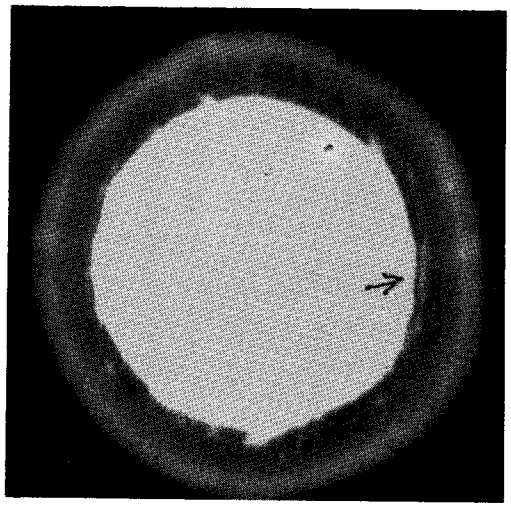

(monolayer 3L–3)

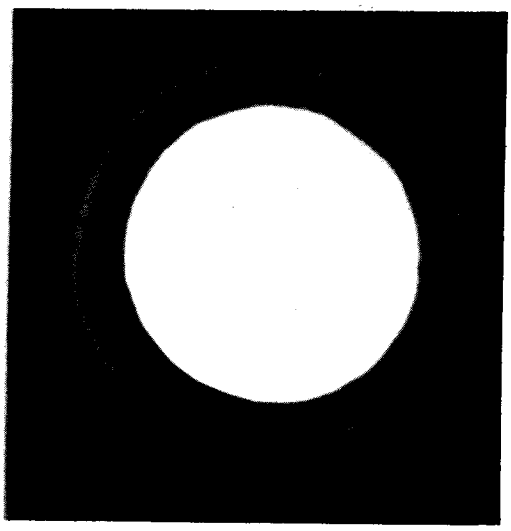

(monolayer 12E–3)

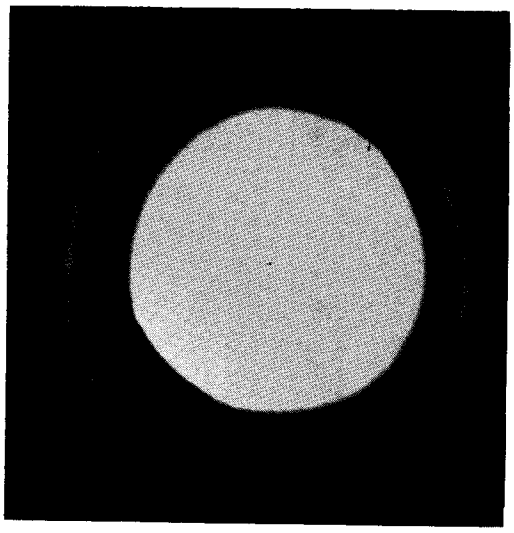

(monolayer 12E–3)

Fig. 23–26 Post-irradiation radiography of particles)

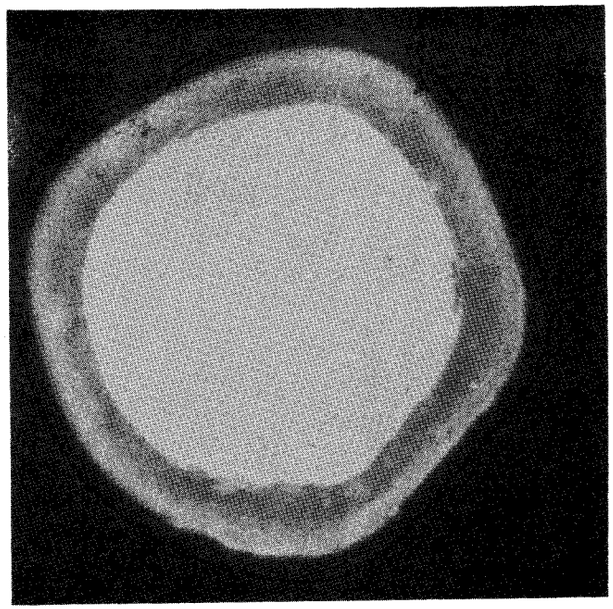

Fig. 27 Post-irradiation radiography of a particle (monolayer C3–77)

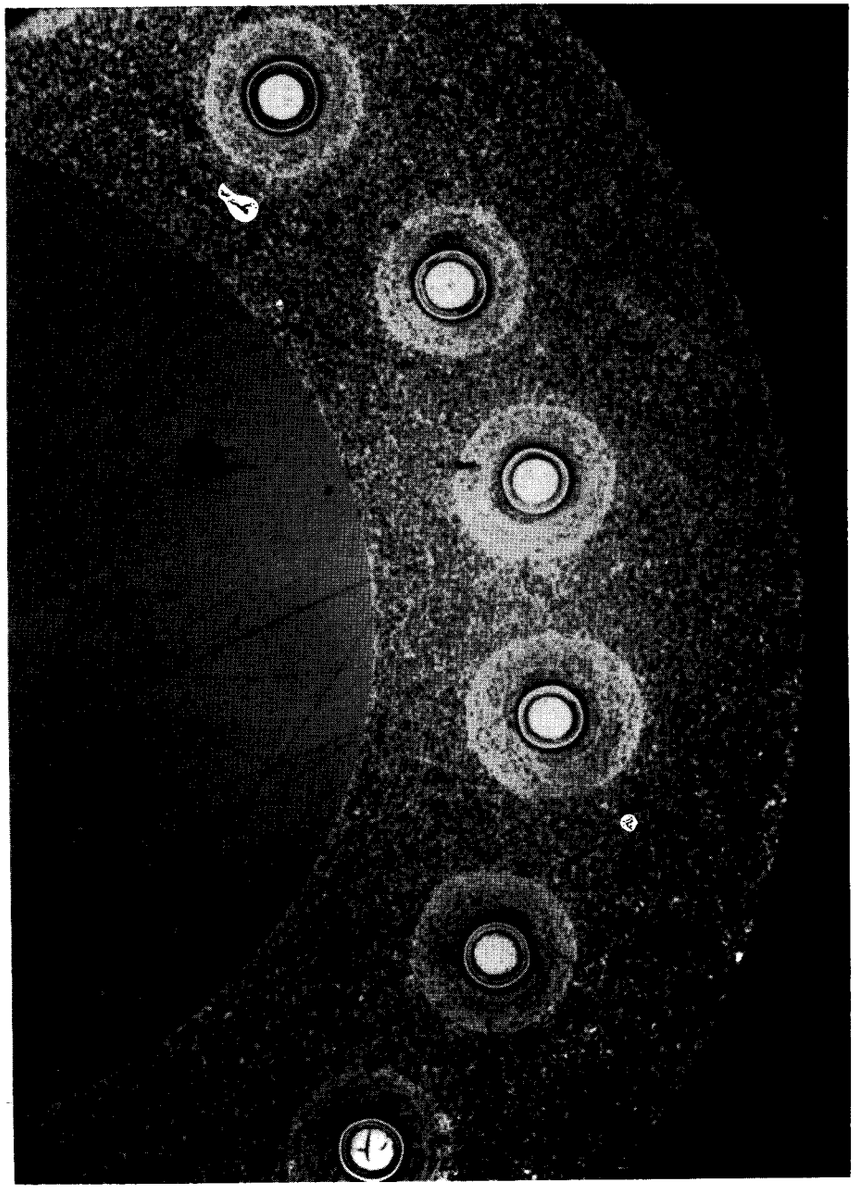

Fig. 28 Ceramography (monolayer 12E–2)

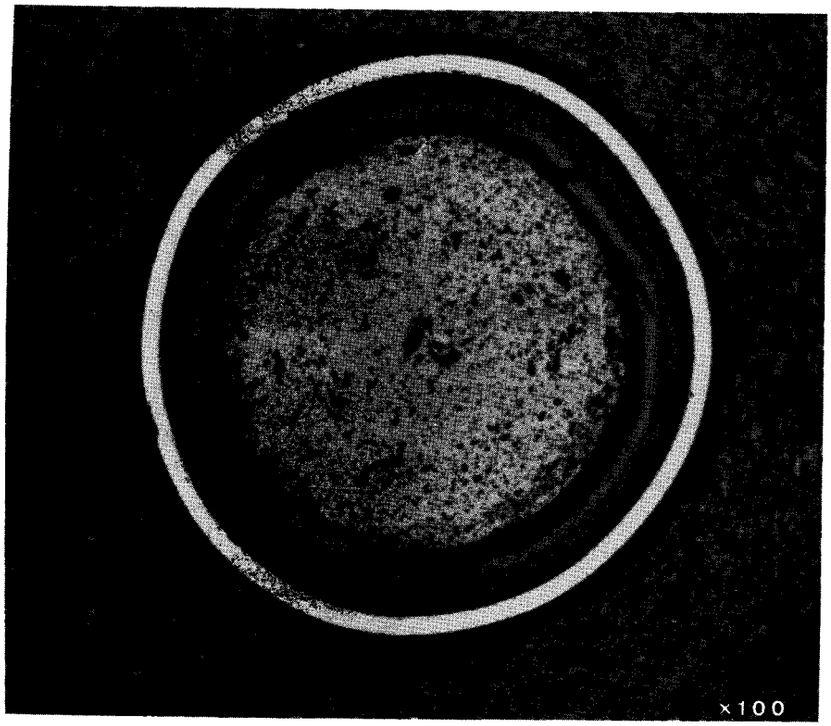

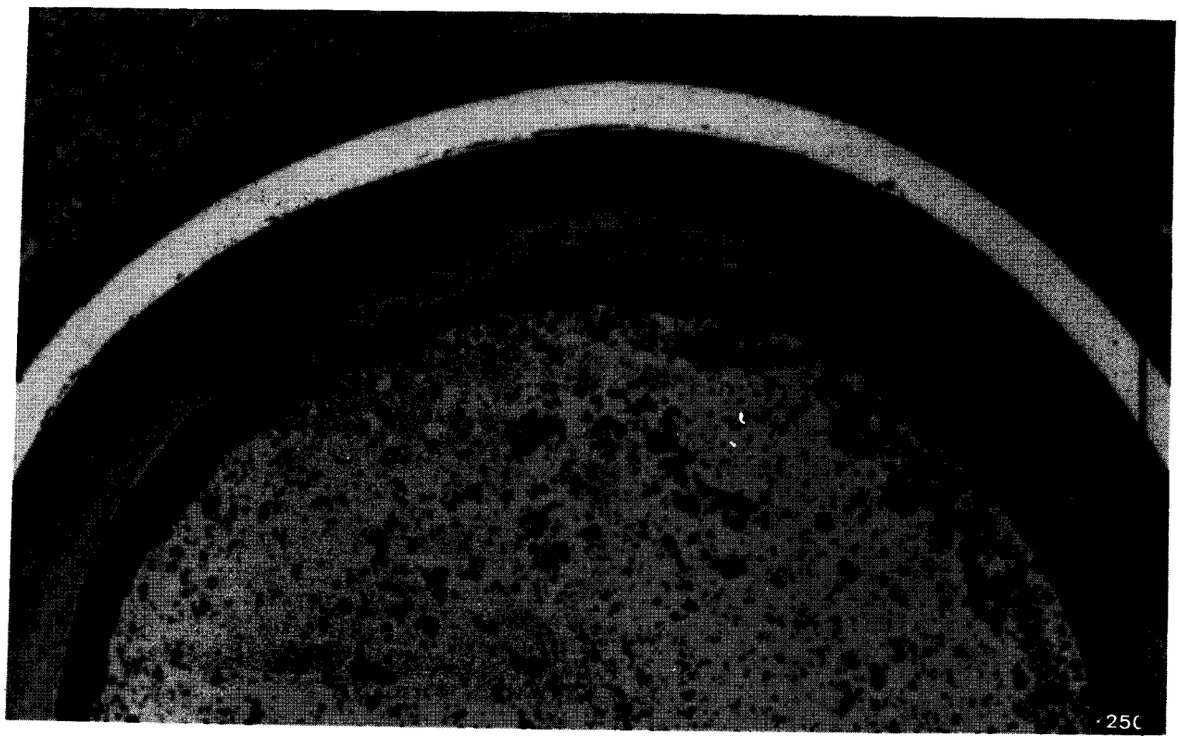

Fig. 29 Ceramography (monolayer 12E–2)

Fig. 30 Ceramography (monolayer 12E–2)

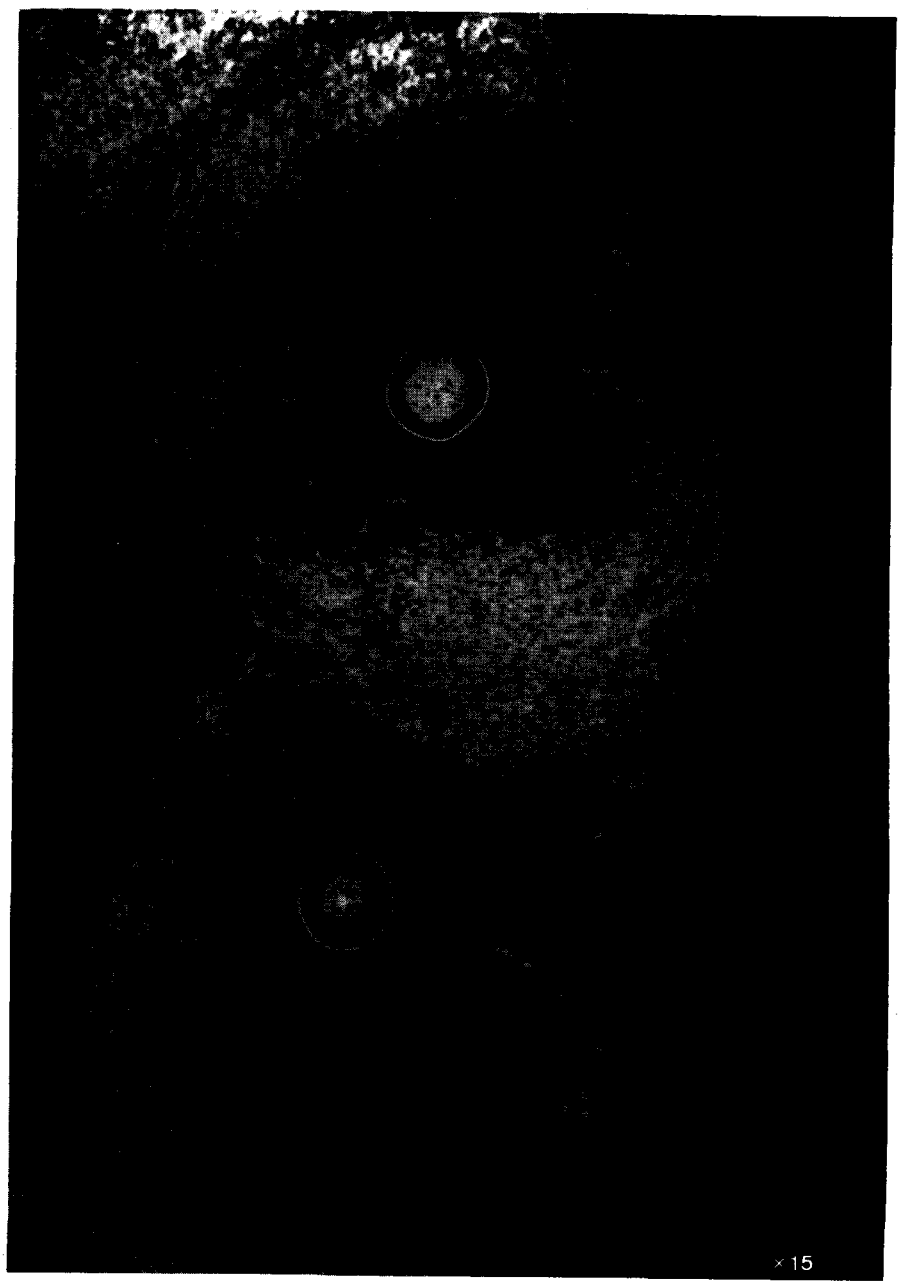

Fig. 31 Ceramography (monolayer K–18)

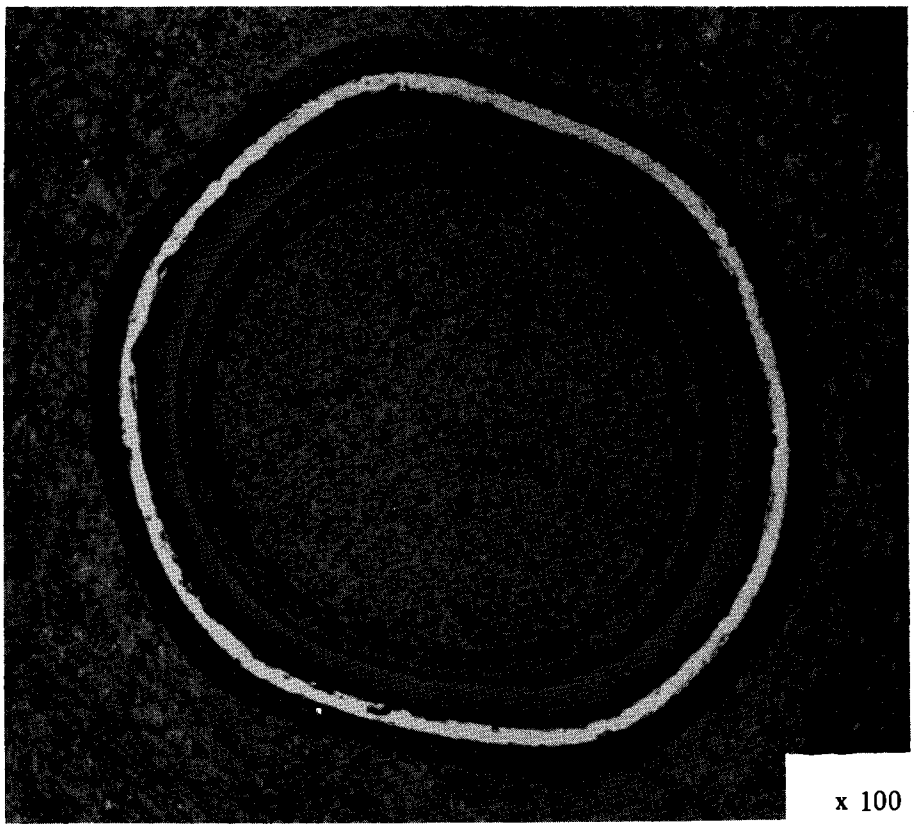

Fig. 32 Ceramography (monolayer K–25)

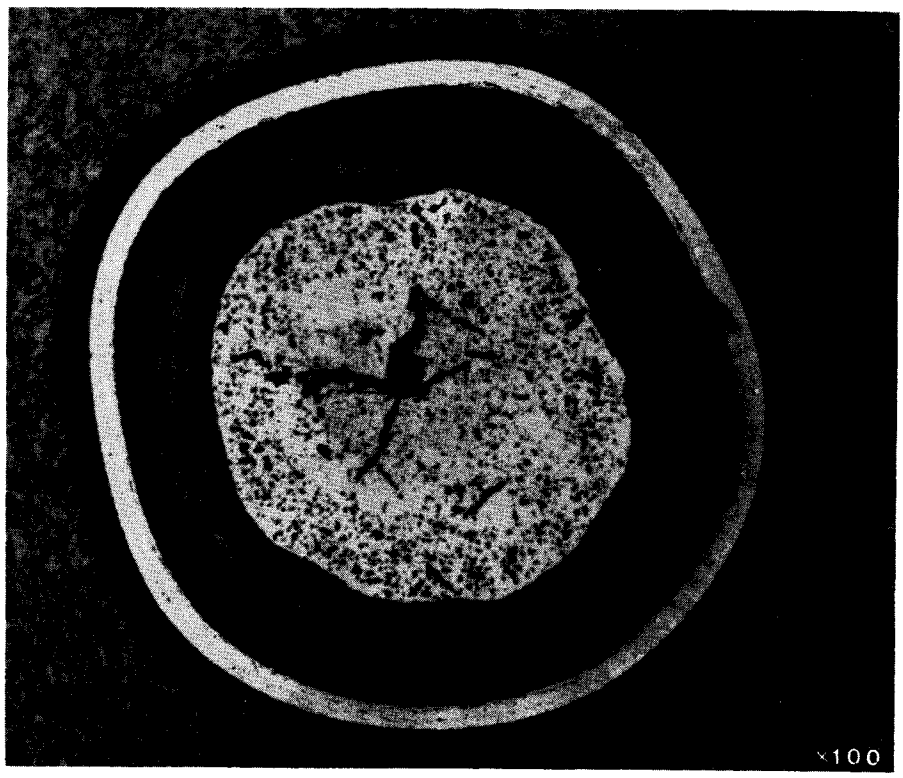

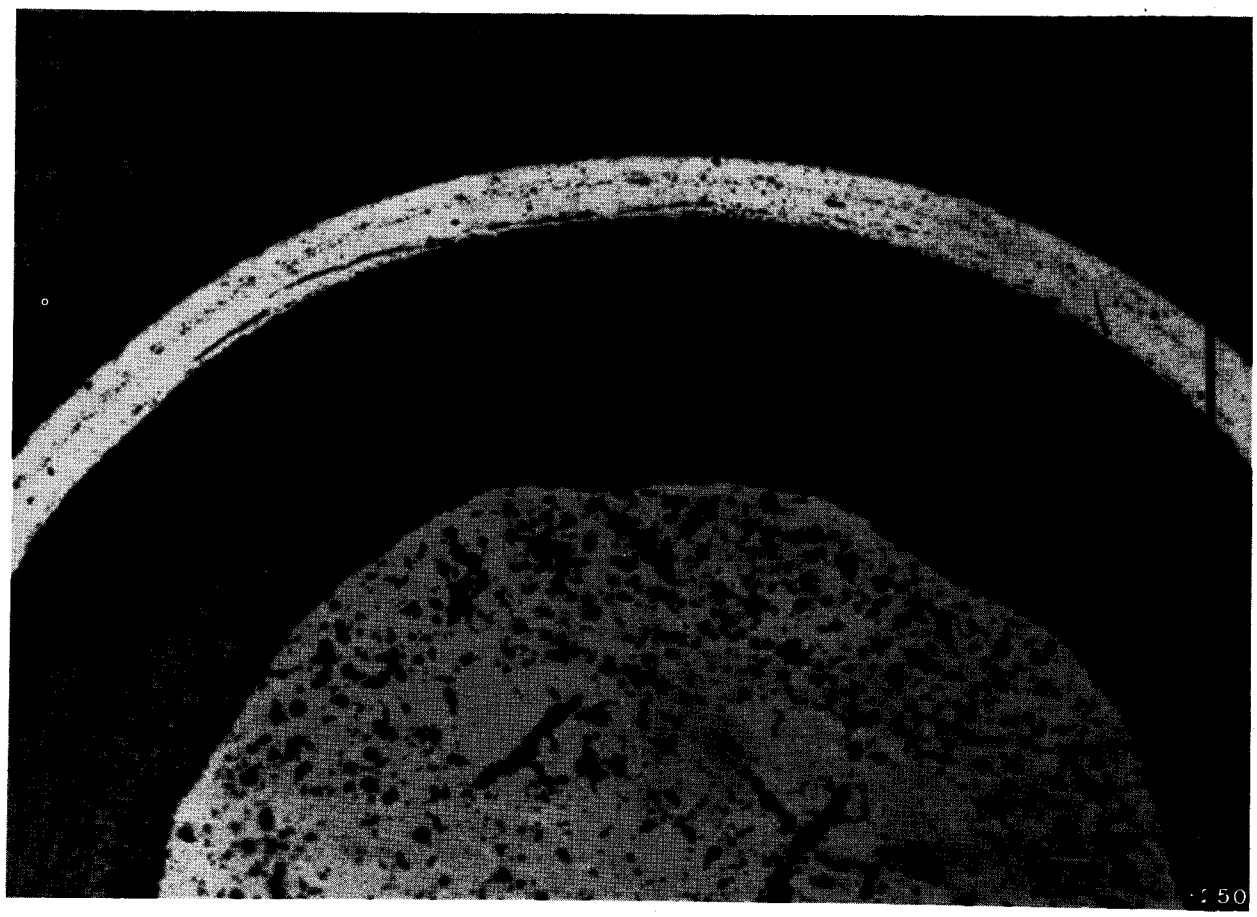

Fig. 33 Ceramography (monolayer 125–2)

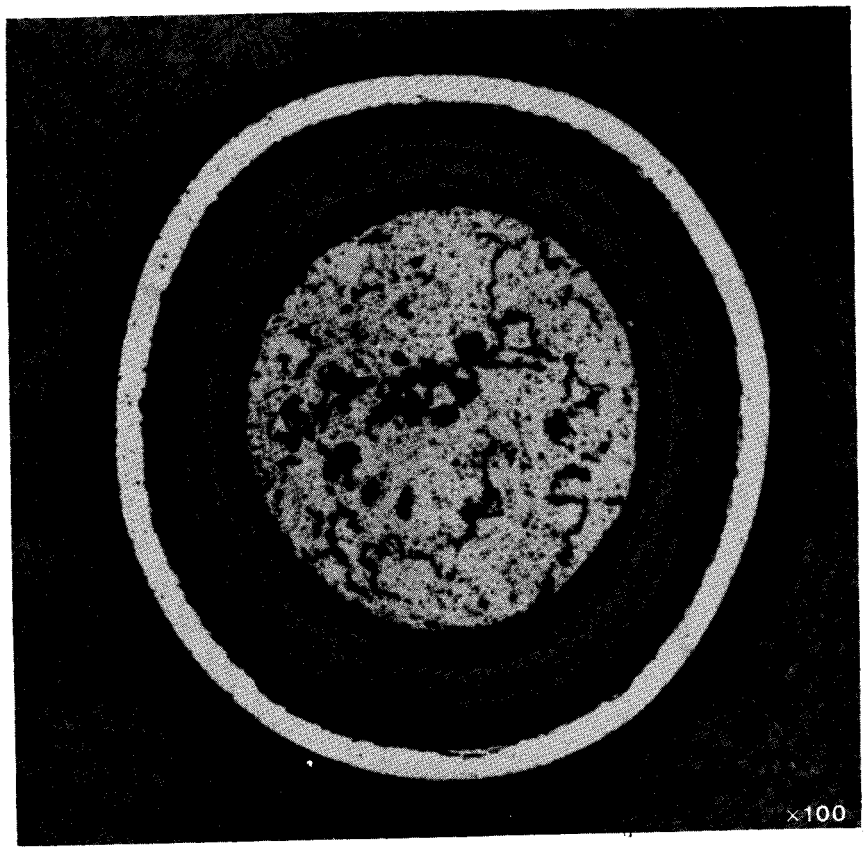

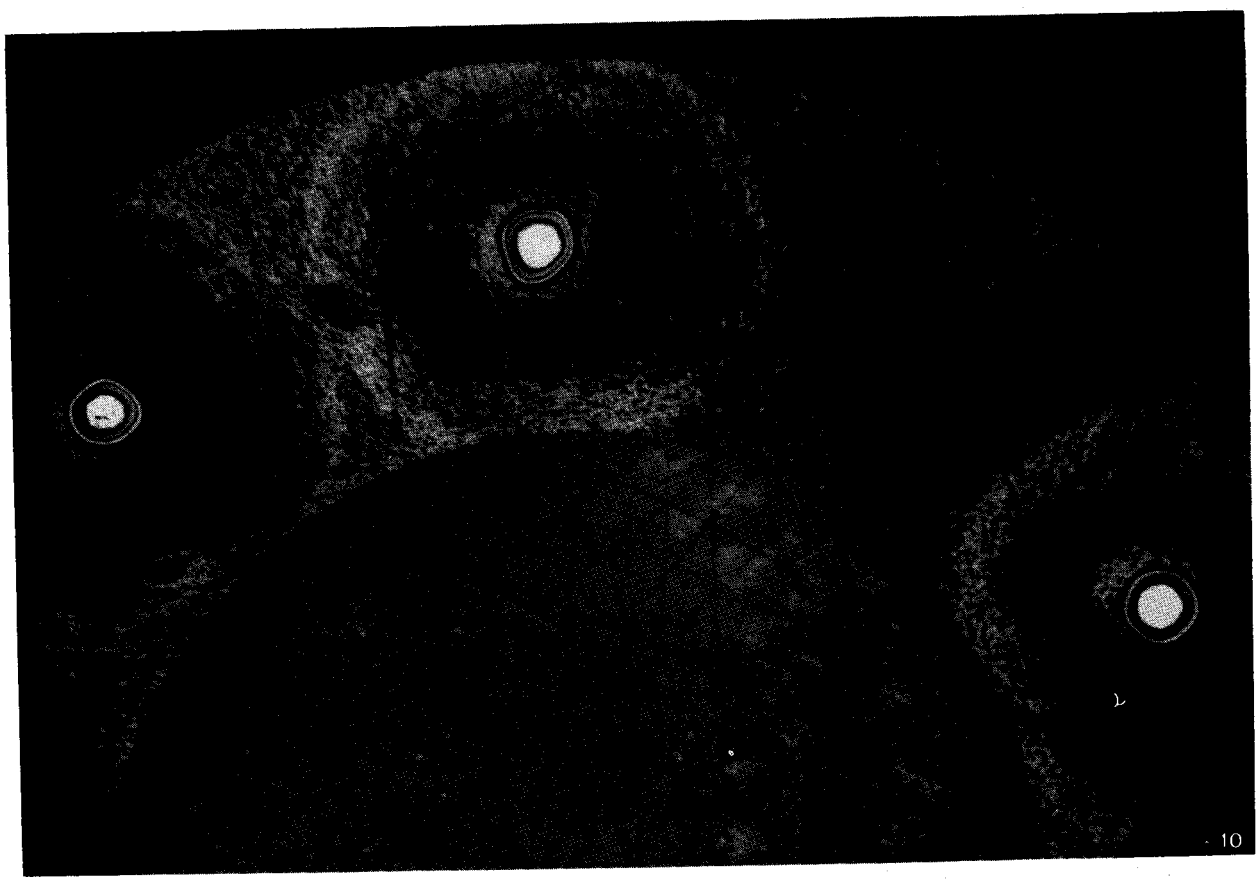

Fig. 34 Ceramography (monolayer 7)

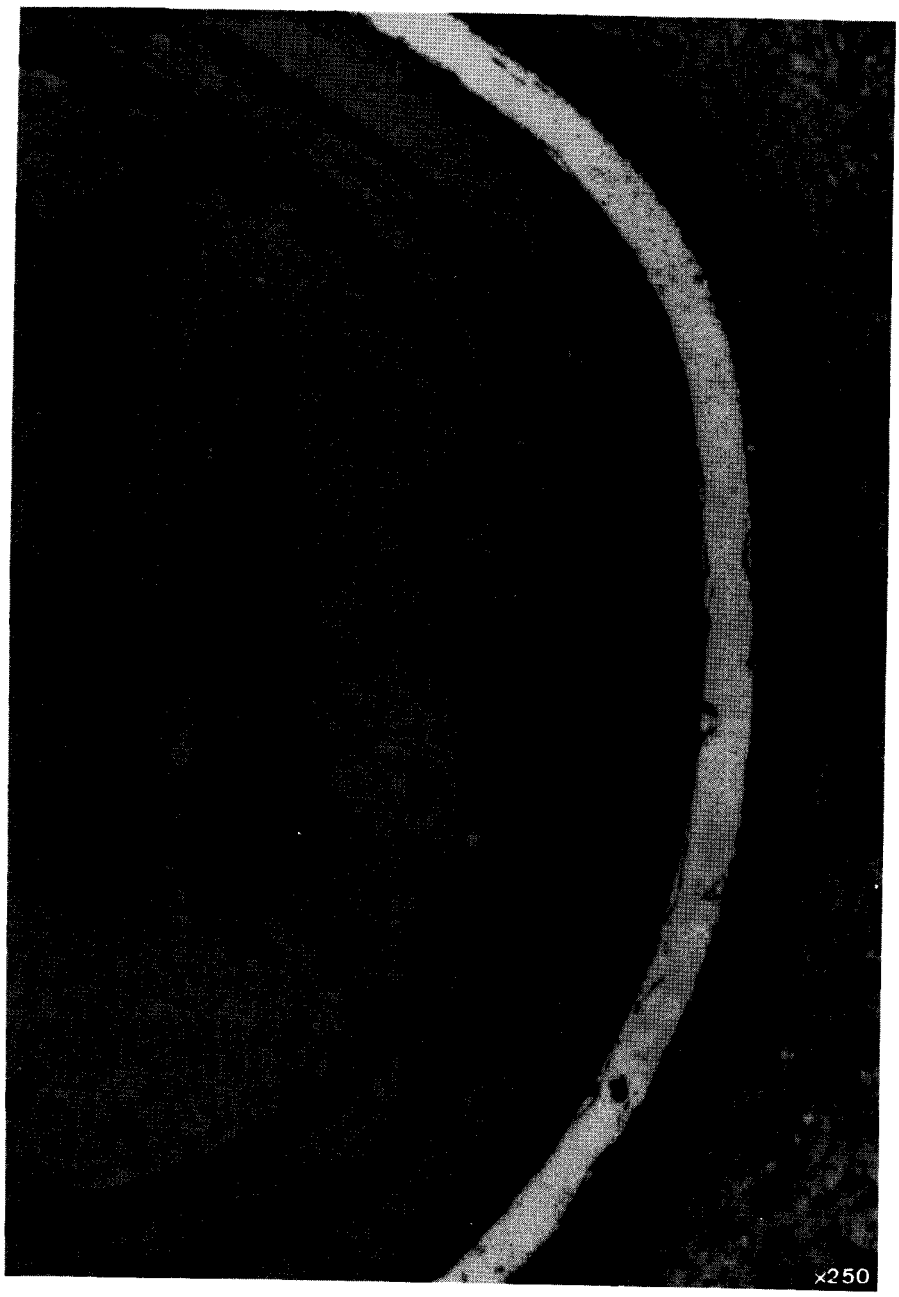

Fig. 35 Ceramography (monolayer K–18)

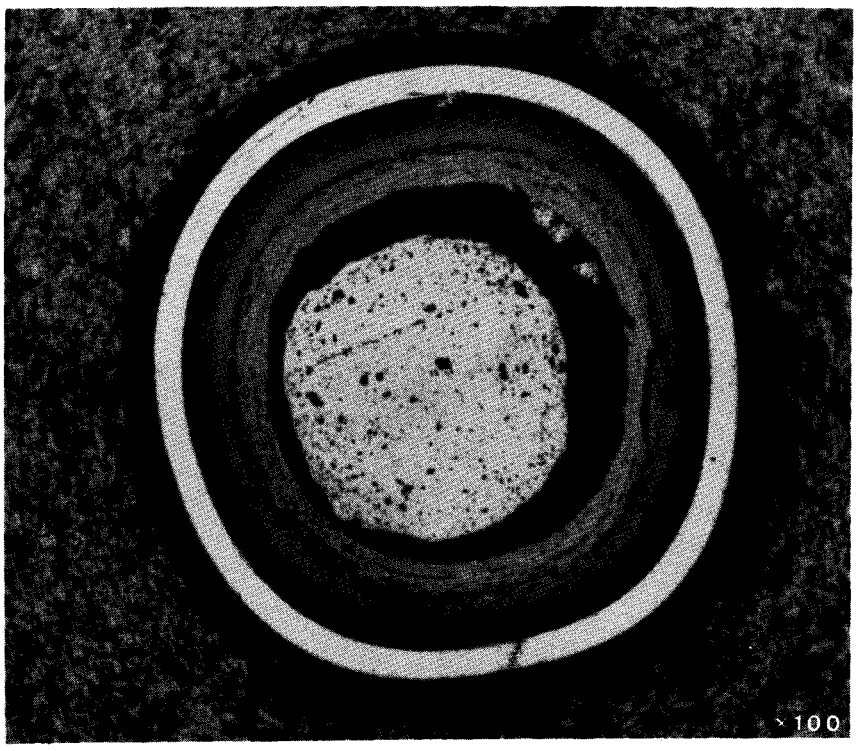

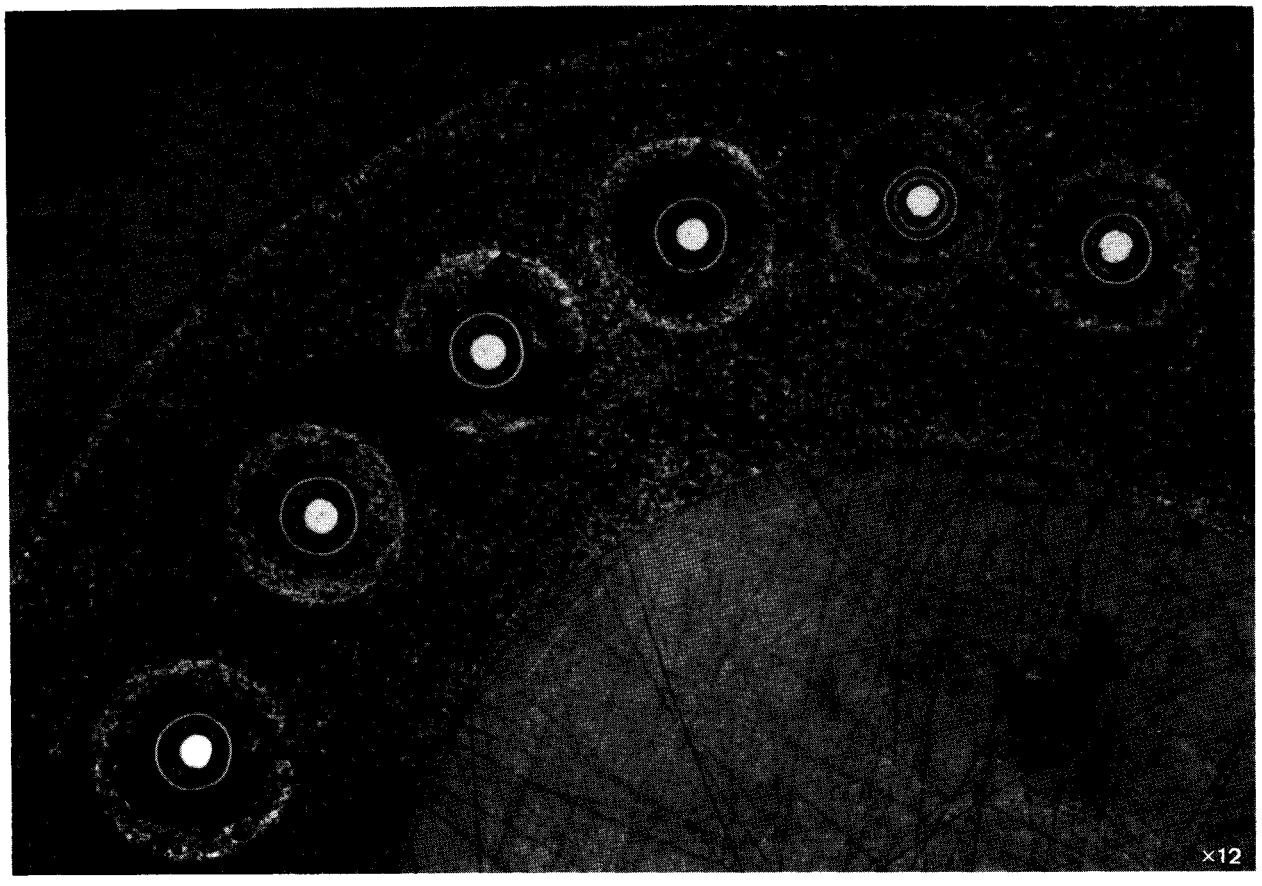

Fig. 36 Ceramography (monolayer 6G–3)

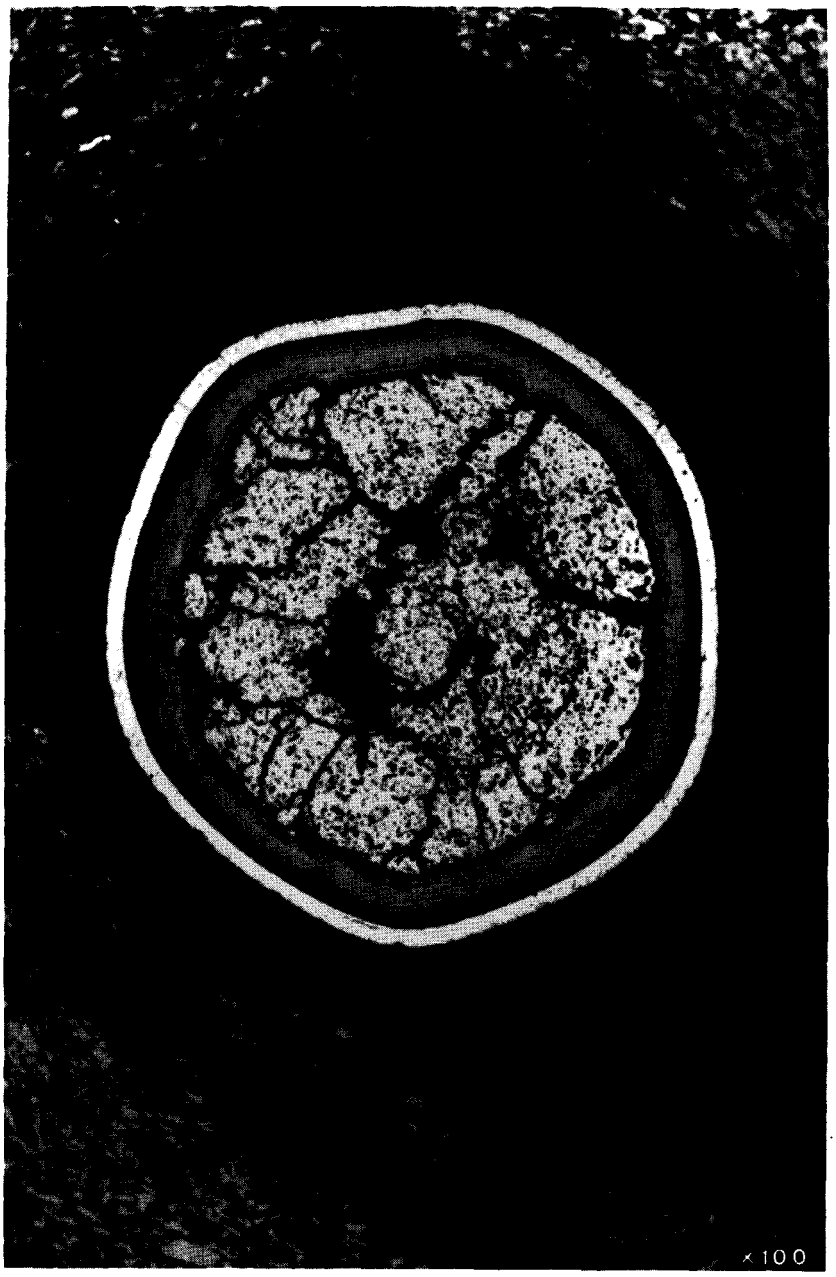

Fig. 37 Ceramography (monolayer 3E)

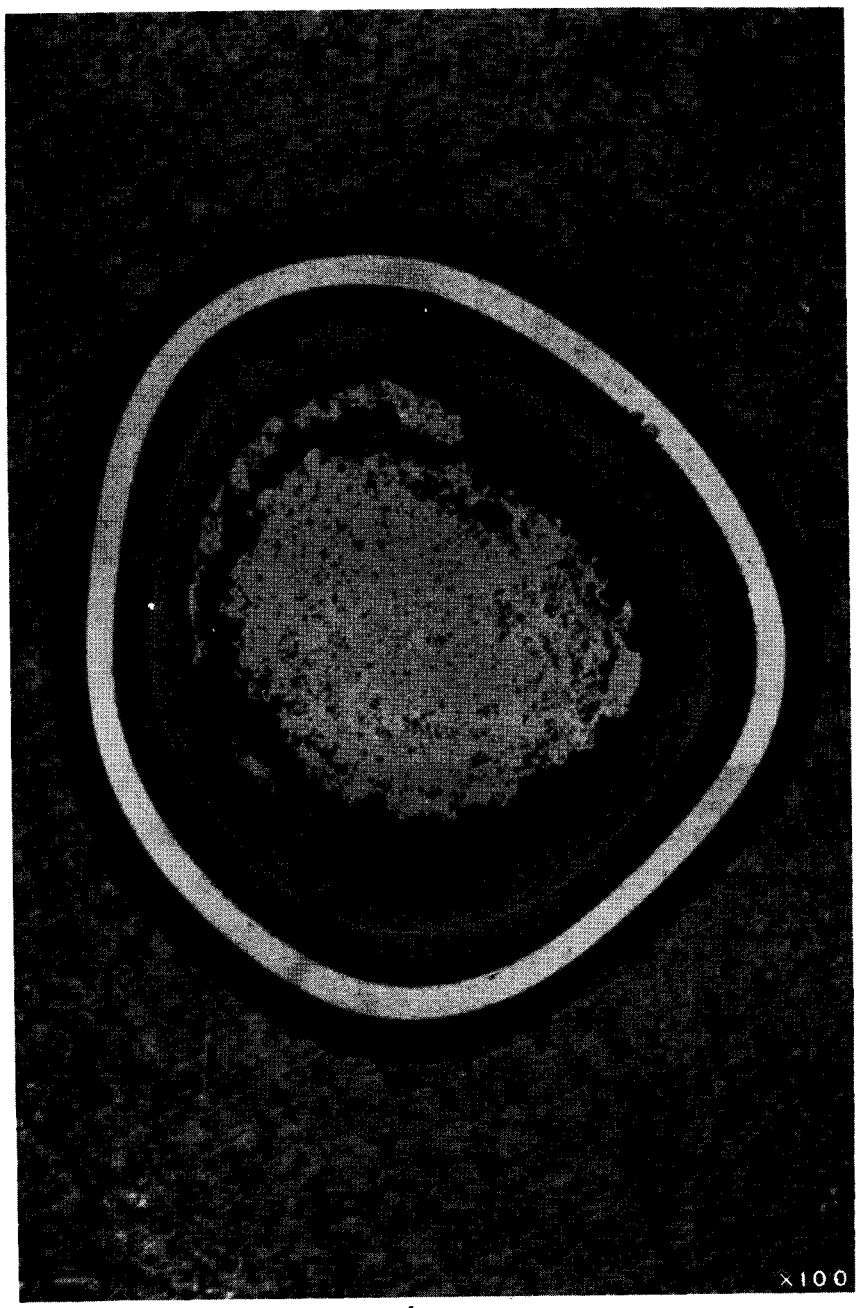

Fig. 38 Ceramography (monolayer 73)

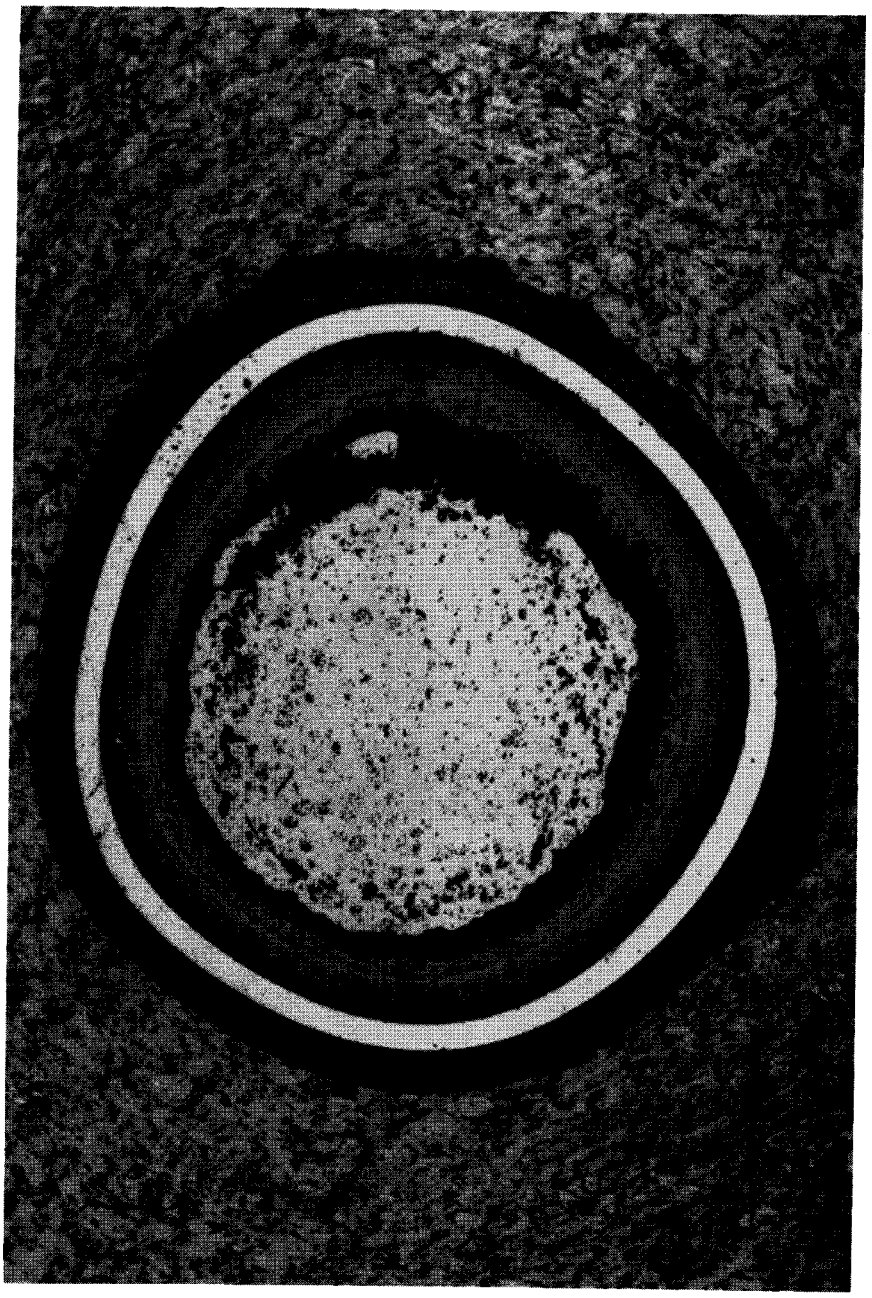

Fig. 39 Ceramography (monolayer 73)

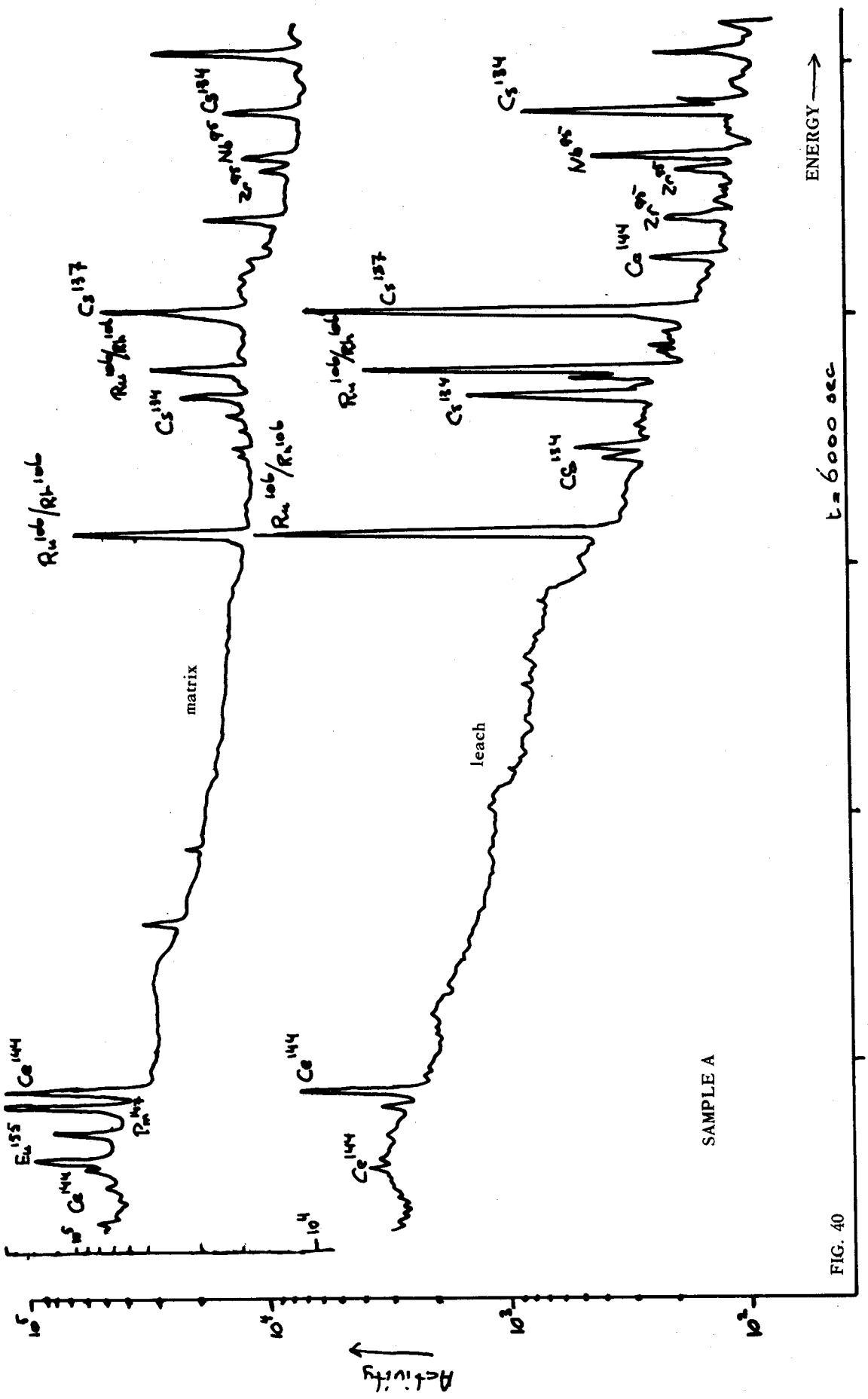
Activity
ENERGY ⟶
t = 6000 sec
matrix
leach
SAMPLE A
Ru106/Rh106
Cs137
Cs134
Ce144
Eu155
Pm147
Zr95 Nb95
Ru106/Rh106
Cs137
Cs134
Ce144
Cs134
Ce144
Cs134
Ce144
Zr95 Nb95
Cs134

FIG. 40

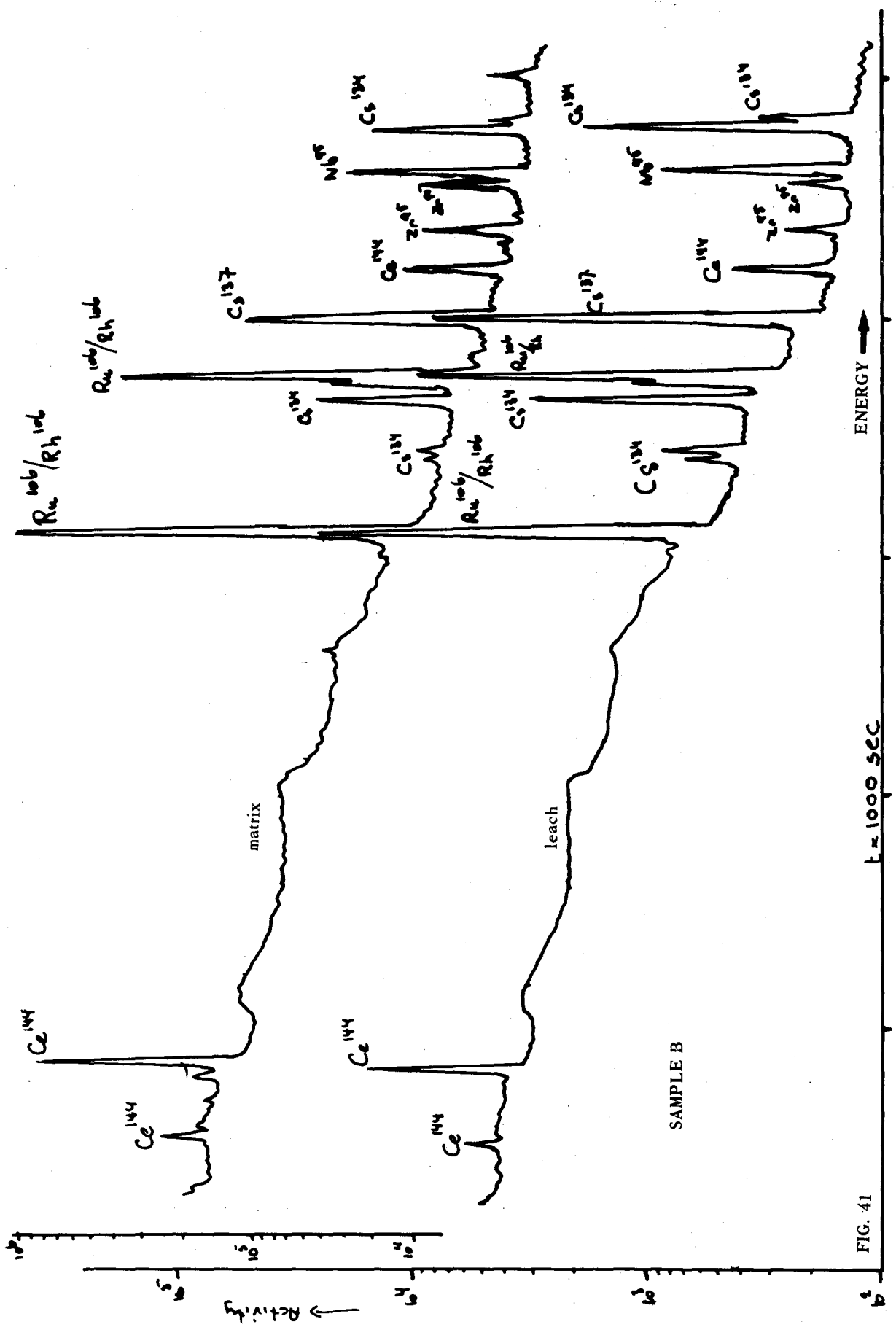
Activity
ENERGY
t = 1000 sec
SAMPLE B
matrix
leach
Ce144
Ru106/Rh106
Cs137
Cs134
Zr95
Nb95
Mn54

FIG. 41

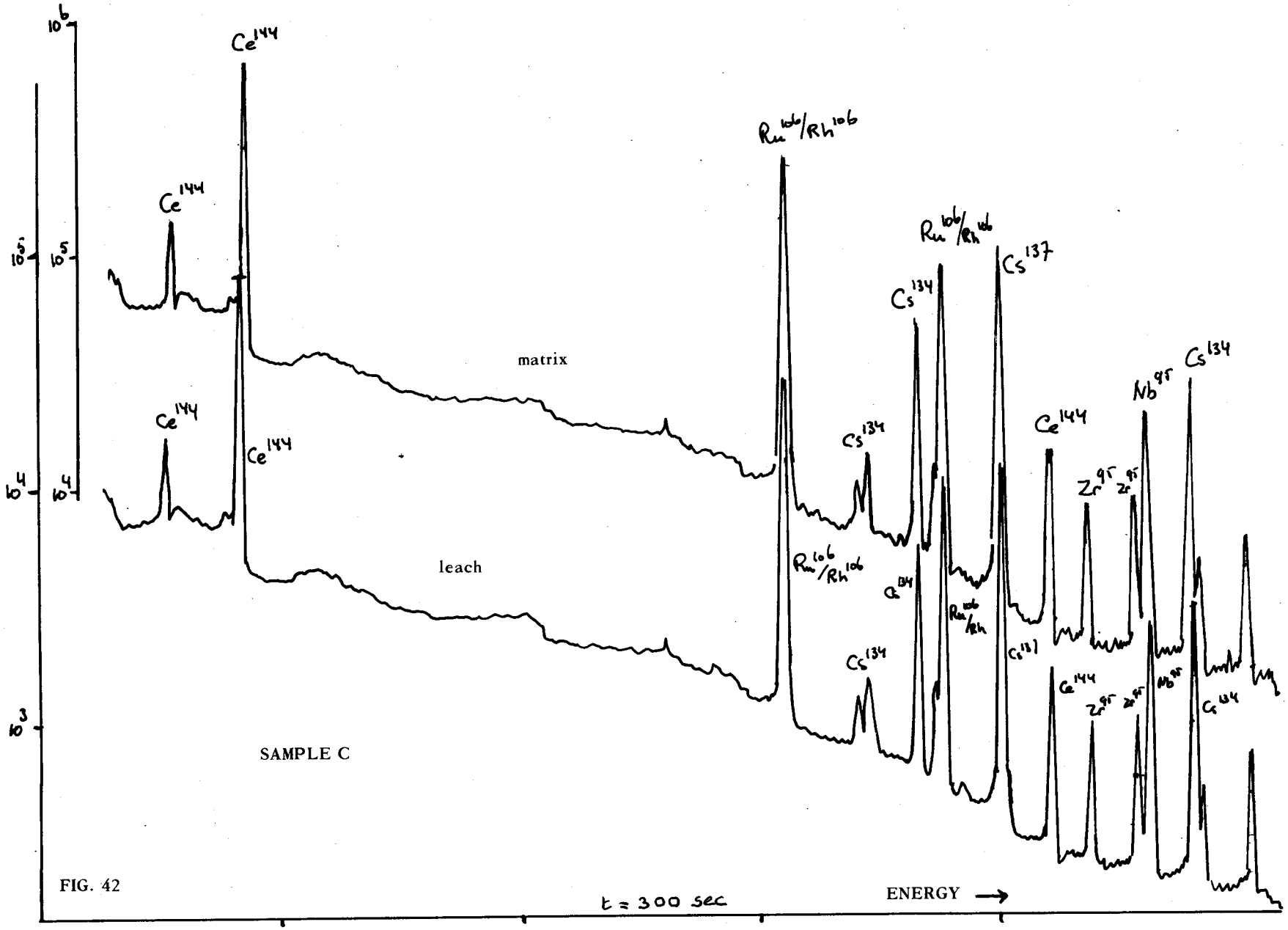
matrix
leach
SAMPLE C
t = 300 sec
ENERGY
Ce144
Ru106/Rh106
Cs134
Cs137
Zr95
Nb95

FIG. 42

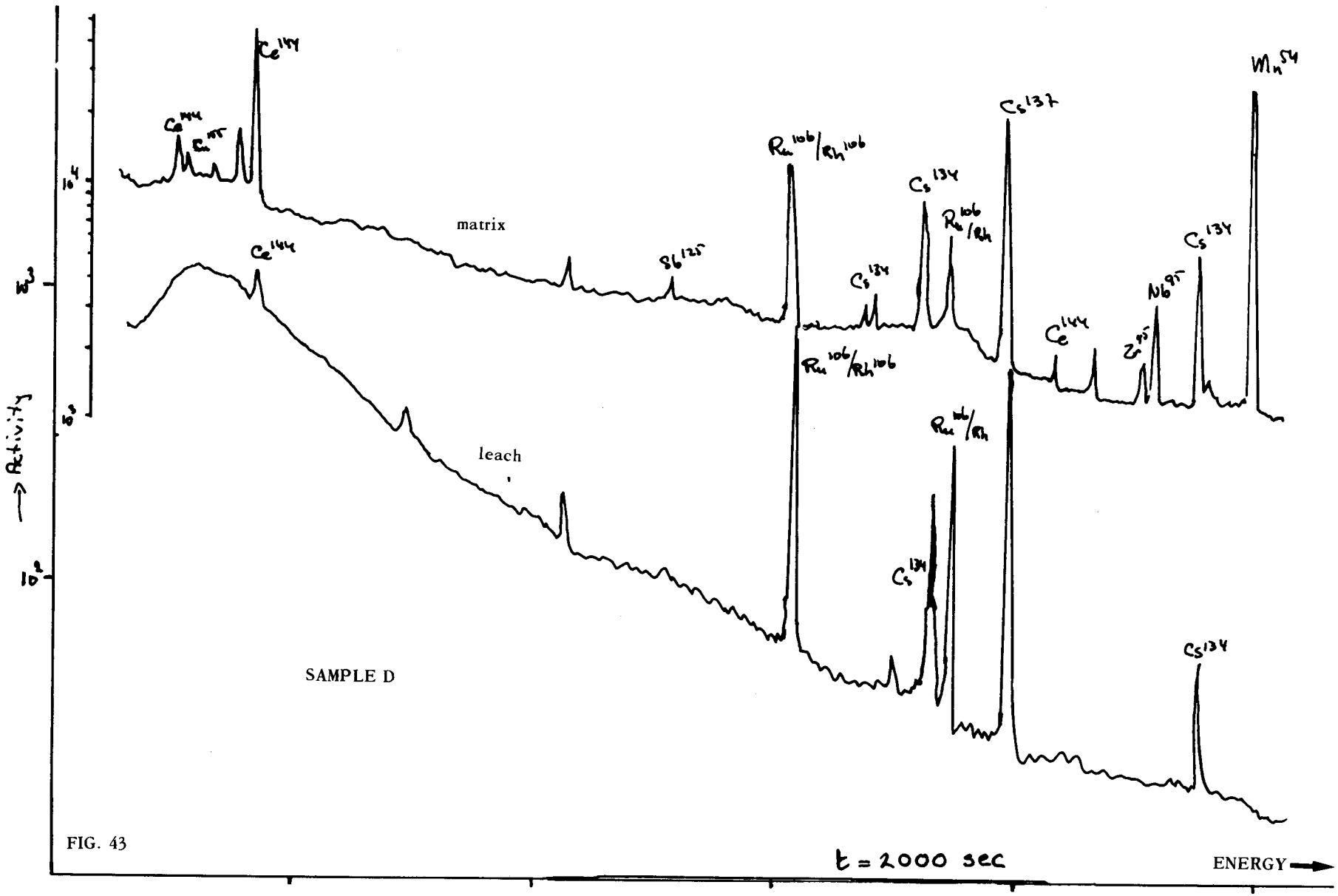
matrix
leach
SAMPLE D
Activity
ENERGY
t = 2000 sec
Ce144
Ru106/Rh106
Cs134
Cs137
Mn54
Sb125
Nb95
Zr95

FIG. 43

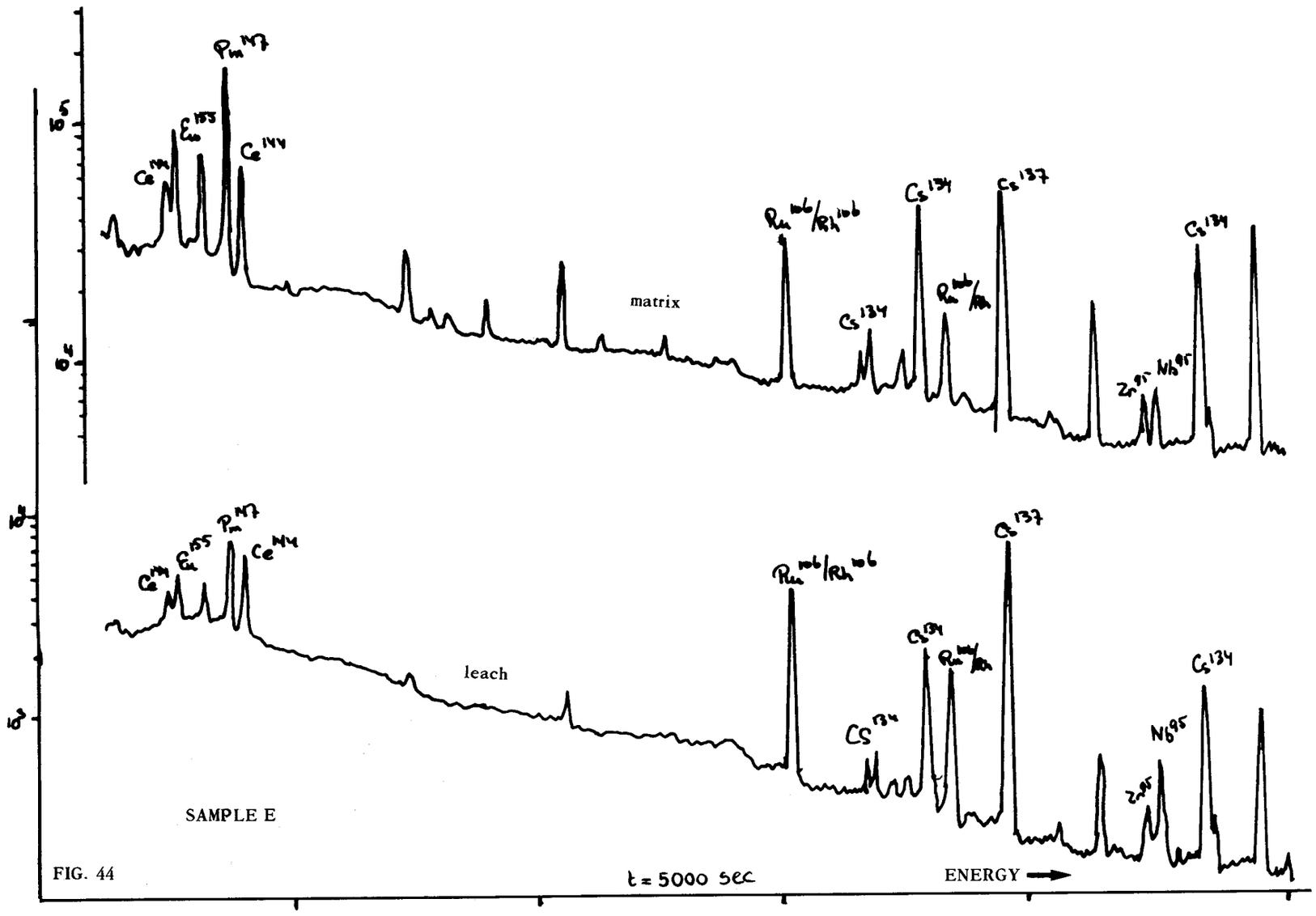

FIG. 44

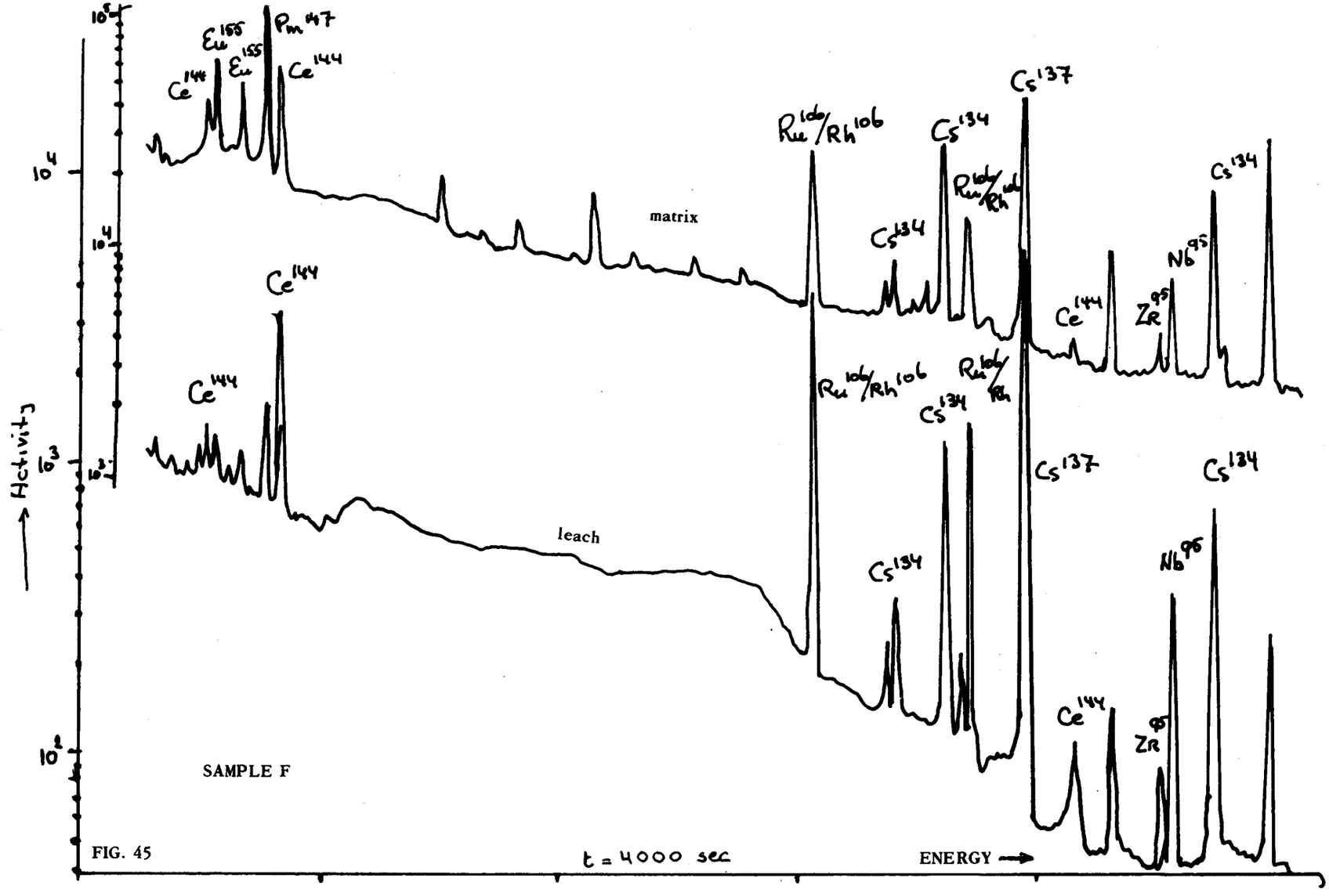
Activity
10^5
10^4
10^3
10^2
Ce^{144}
Eu^{155}
Pm^{147}
Ce^{144}
matrix
Ru^{106}/Rh^{106}
Cs^{134}
Cs^{137}
Cs^{134}
Ce^{144}
Zr^{95}
Nb^{95}
Cs^{134}
Ce^{144}
Ce^{144}
leach
Ru^{106}/Rh^{106}
Cs^{134}
Cs^{137}
Cs^{134}
Cs^{134}
Nb^{95}
Ce^{144}
Zr^{95}
SAMPLE F
t = 4000 sec
ENERGY

FIG. 45

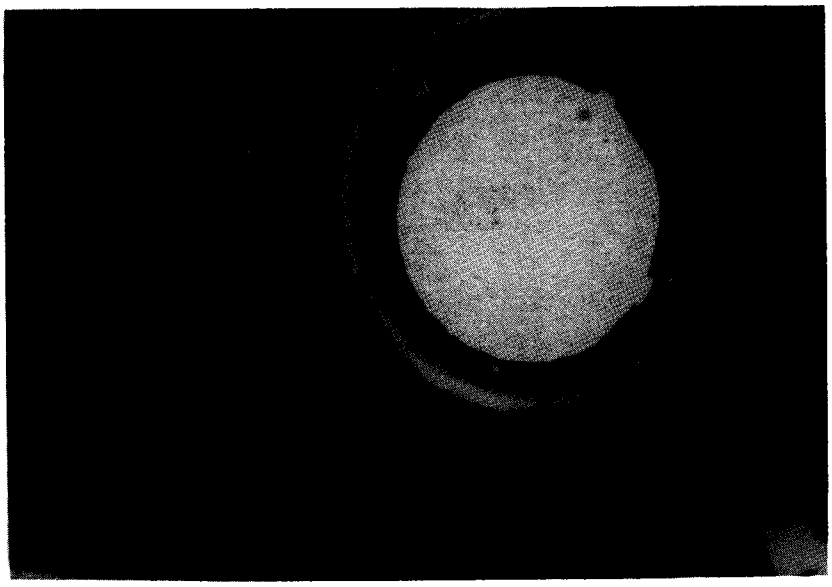

Fig. 46 Radiography of fragments of coating (irradiated samples)

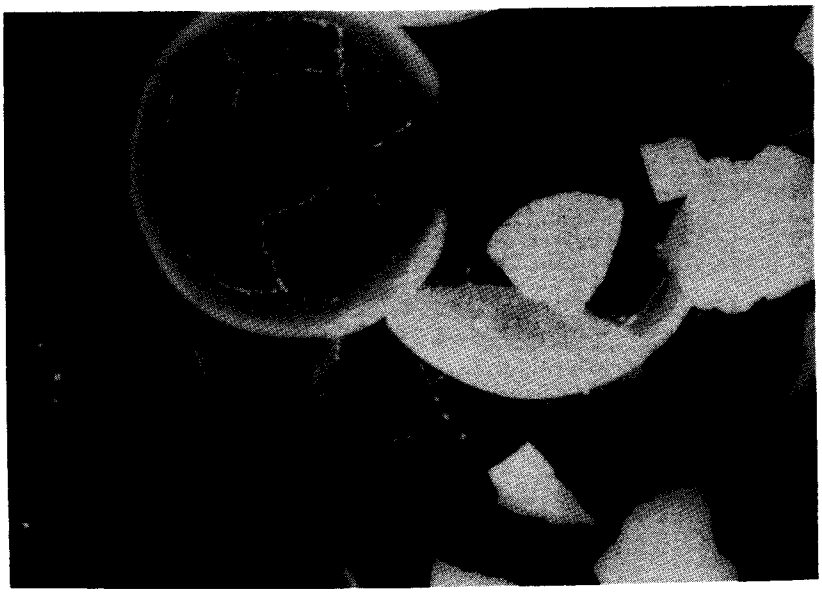

Fig. 47 Radiography of a broken irradiated particle.

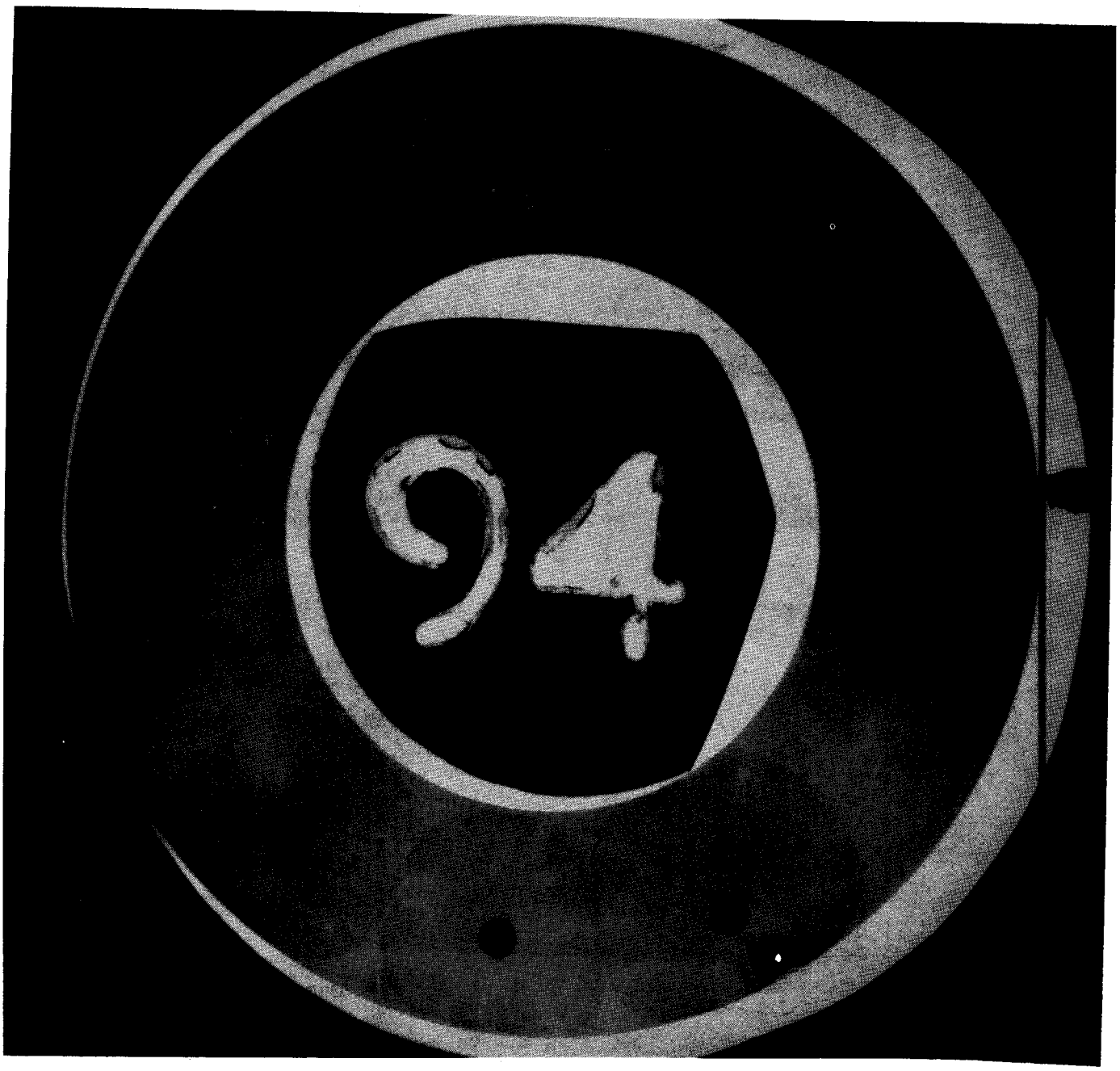

Fig. 48 Radiography of a monolayer before the irradiation showing the overcoating with radial crack generated during the compression of the matrix.

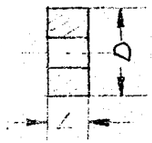

Dimensional measurements

Irradiation test E 96-01

TABLE I

D means Diameter before irradiation in mm Accuracy ± 0,02
D' " " after " " " " ± 0,02
L means Length before irradiation in mm Accuracy ±0,04 −0,02
L' " " after " " " " ±0,04 −0,02

Company	Sample N°	Box N°	Length (mm)		diameter (mm)				Remarks
							Sample 90°turned		
			L	L'	D	D'	D	D'	
Dragon	3L1	I	1,97	1,96	21,96	21,86	21,96	21,86	
	12L5		1,99	1,97	21,96	21,86	21,96	21,86	
	6G1		1,99	1,96	21,97	21,86	21,96	21,86	
	3G1		2,01	,95	21,97	21,86	21,97	21,86	
	122-1		1.97	1,95	21,97	21,85	21,97	21,85	
	12E1		1,98	1,97	21,96	21,84	21,96	21,84	
	3E1		1,99	1,97	21,95	21,84	21,96	21,84	
	129-5		2,00	1,97	21,95	21,85	21,95	21,84	
	6C7		1.97	1,95	21,96	21,85	21,96	21,84	
	3C1		1,99	1,98	21,97	21,85	21,97	21,85	
	125-1		2,00	1,95	21,97	21,85	21,97	21,85	
	3A1		1,98	1,94	21,96	21,85	21,96	21,85	
	6A6		1,95	1,95	21,96	21,85	21,96	21,85	
	6A1C				21,97	21,85	21,97	21,85	Compact.

Dimensional measurements
Irradiation test E 96-01

TABLE II

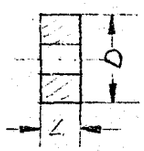

D means Diameter before irradiation in mm Accuracy ± 0,02
D' " " after " " " " ± 0,02
L means Length before irradiation in mm Accuracy $^{+0,04}_{-0,02}$
L' " " after " " " " $^{+0,04}_{-0,02}$

Company	Sample N°	Box N°	Length (mm)		diameter (mm)				Remarks
							Sample 90°turned		
			L	L'	D	D'	D	D'	
K.F.A.	K 1	I	1,96		21,95	21,85	21,97	21,85	
	K 2		2,02		21,95	21,85	21,96	21,85	
	K 4		1.96		21,95	21,85	21,96	21,85	
	K 6		2,16		21,95	21,85	21,96	21,85	
	K 7		2,00		21,95	21,84	21,95	21,84	
	K 8		1,98		21,95	21,84	21,95	21,84	
	K 9		1,87		21,95	21,82	21,95	21,82	
	K10		2,10		21,95	21,79	21,95	21,80	
	K11		2,02		21,96	21,83	21,95	21,82	
	K12		2,05		21,96	21,83	21,95	21,83	
	K13		1,98		21,96	21,83	21,95	21,83	
	K15		2,01		21,96	21,84	21,95	21,84	

Dimensional measurements

Irradiation test E 96-01

TABLE III

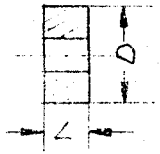

D means Diameter before irradiation in mm Accuracy ± 0,02
D' " " after " " " " ± 0,02
L means Length before irradiation in mm Accuracy +0,04 −0,02
L' " " after " " " " +0,04 −0,02

Company	Sample N°	Box N°	Length (mm)		diameter (mm)				Remarks
							Sample 90°turned		
			L	L'	D	D'	D	D'	
Bel.Nuc.	66	I	2,04		21,79	21,81	21,79	21,81	
	67		2,03		21,79	21,80	21,79	21,80	
	21		2,19		21,83	21,78	21,84	21,78	
	37		10,12		21,82	21,73	21,83	21,73	Compact
	87		2,09		21,84	21,75	21,85	21,75	
	38		10,12		21,83	21,74	21,85	21,74	Compact
	4		2,09		21,83	21,71	21,84	21,71	
	43		10,10		21,83	21,75	21,84	21,75	Compact

Dimensional measurements

Irradiation test E 96-01

TABLE IV

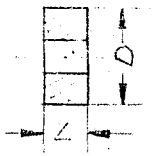

D means Diameter before irradiation in mm Accuracy ± 0,02
D' " " after " " " " ± 0,02
L means Length before irradiation in mm Accuracy +0,04 −0,02
L' " " after " " " " +0,04 −0,02

Company	Sample N°	Box N°	Length (mm)		diameter (mm)				Remarks
			L	L'	D	D'	Sample 90°turned D	Sample 90°turned D'	
Dragon	3L2	II	1,96		21,98	21,79	21,97	21,79	
	12L6		2,00		21,97	21,79	21,97	21,79	
	6G5		2,00		21,97	21,79	21,97	21,79	
	3G7		1,98		21,98	21,79	21,98	21,79	
	122-2		1,99		21,97	21,78	21,97	21,78	
	12E2		1,98		21,97	21,78	21,97	21,78	
	3E5		1,98		21,97	21,77	21,97	21,77	
	129-2		1,99		21,95	21,75	21,95	21,75	
	6C2		1,98		21,95	21,77	21,94	21,77	
	3C2		2,00		21,95	21,77	21,95	21,77	
	125-2		1,95		21,95	21,77	21,95	21,77	
	3A2		1,99		21,96	21,77	21,96	21,77	
	6A2		1,98		21,96	21,77	21,97	21,77	
	6A2C		13,74		21,97	21,77	21,96	21,77	Compact

Dimensional measurements
Irradiation test E 96-01

TABLE V

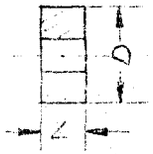

D means Diameter before irradiation in mm Accuracy ± 0,02
D " " after " " " " ± 0,02
L means Length before irradiation in mm Accuracy +0,04 −0,02
L' " " after " " " " +0,04 −0,02

Company	Sample N°	Box N°	Length (mm)		diameter (mm)				Remarks
							Sample 90°turned		
			L	L'	D	D'	D	D'	
K.F.A.	K17	II	1,84		21,96	21,78	21,96	21,78	
	K18		1,92		21,96	21,79	21,96	21.79	
	K20		2,16		21,95	21,81	21,96	21,81	
	K21		2,11		21,96	21,81	21,95	21,81	
	K23		2,05		21,96	21.81	21,96	21,81	
	K24		2,01		21,96	21,81	21,96	21,81	
	K25		1,91		21,95	21,81	21,96	21,81	
	K27		2,11		21,95	21,81	21,96	21,81	
	K31		2,02		21,95	21,81	21,96	21,81	
	K32		2,09		21,95	21,81	21,96	21,81	
	K33		1,98		21,95	21,81	21,96	21,81	
	K36		2,19		21,95	21,81	21,96	21,81	

Dimensional measurements

Irradiation test E 96-01

TABLE VI

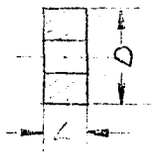

D means Diameter before irradiation in mm Accuracy ± 0,02
D' " " after " " " " ± 0,02
L means Length before irradiation in mm Accuracy +0,04 −0,02
L' " " after " " " " +0,04 −0,02

Company	Sample N°	Box N°	Length (mm)		diameter (mm)				Remarks
							Sample 90°turned		
			L	L'	D	D'	D	D'	
Bel.Nuc.	68	II	1,98		21,81	21,81	21,81	21,81	
	22		2,05		21,80	21,79	21,79	21,79	
	55		10,00		21,82	21,75	21,81	21,75	Compact
	90		2,04		21,82	21,75	21,82	21,75	
	56		10,07		21,81	21,75	21,82	21,75	Compact
	7		2,07		21,81	21,73	21,81	21,73	
	73		2,08		21,79	21,68	21,79	21,68	
	44		10,12		21,81	21,75	21,81	21,75	Compact

Dimensional measurements

Irradiation test E 96-01

TABLE VII

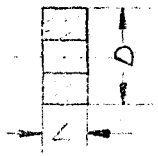

D means Diameter before irradiation in mm Accuracy ± 0,02
D' " " after " " " " ± 0,02
L means Length before irradiation in mm Accuracy +0,04 −0,02
L' " " after " " " " +0,04 −0,02

Company	Sample N°	Box N°	Length (mm)		diameter (mm)				Remarks
							Sample 90°turned		
			L	L'	D	D'	D	D'	
Dragon	3L3	III	1,98		21,97	21,77	21,97	21,77	
	12L7		1,98		21,97	21,77	21,97	21,77	
	6G3		1,98		21,98	21,77	21,97	21,77	
	3G3		1,99		21,98	21,76	21,97	21,76	
	122-3		1,98		21,97	21,75	21,97	21,75	
	12E3		1,98		21,96	21,75	21,96	21,75	
	3E3		1,97		21,95	21,74	21,95	21,74	
	129-3		2,00		21,95	21,74	21,95	21,74	
	6C3		2,00		21,95	21,76	21,95	21,76	
	3C3		1,97		21,96	21,76	21,96	21,76	
	125-6		1,97		21,96	21,76	21,96	21,76	
	3A3		1,97		21,96	21,76	21,96	21,76	
	6A3		1,97		21,96	21,76	21,96	21,76	
	6A3C		13,86		21,97	21,76	21,97	21,76	Compact.

Dimensional measurements

Irradiation test E 96-01

TABLE VIII

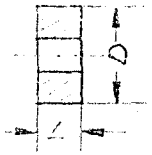

D means Diameter before irradiation in mm Accuracy ± 0,02
D' " " after " " " " ± 0,02
L means Length before irradiation in mm Accuracy +0,04 −0,02
L' " " after " " " " +0,04 −0,02

Company	Sample N°	Box N°	Length (mm)		diameter (mm)				Remarks
			L	L'	D	D'	Sample 90°turned D	Sample 90°turned D'	
K.F.A.	K39	III	1,98		21,95	21,77	21,96	21.77	
	K40		1,91		21,96	21,82	21,96	21,82	
	K41		2,22		21,96	21,82	21,96	21,82	
	K42		1,93		21,96	21,83	21,96	21.83	
	K44		1,92		21,96	21,82	21,96	21,82	
	K45		2,06		21,95	21,82	21,96	21,82	
	K48		2,03		21,95	21,82	21,96	21,82	
	K50		1,96		21,95	21,81	21,96	21,81	
	K52		2,10		21,95	21,81	21.96	21,81	
	K53		2,00		21,96	21,82	21,96	21,82	
	K54		2,12		21,96	21,82	21,96	21,82	
	K55		1,99		21,95	21,81	21,96	21,81	

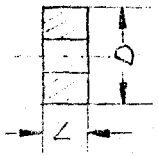

Dimensional measurements
Irradiation test E 96-01

TABLE IX

D means Diameter before irradiation in mm Accuracy ± 0,02
D' " " after " " " " ± 0,02
L means Length before irradiation in mm Accuracy $^{+0,04}_{-0,02}$
L' " " after " " " " $^{+0,04}_{-0,02}$

Company	Sample N°	Box N°	Length (mm)		diameter (mm)				Remarks
							Sample 90°turned		
			L	L'	D	D'	D	D'	
Bel.Nuc	11	III	2,03		21,81	21,80	21,81	21,80	
	77		2,12		21,80	21,80	21,80	21,80	
	92		2,05		21,79	21,75	21,70	21,75	
	74		2,04		21,79	21,69	21,79	21,69	
	23		2,05		21,79	21,68	21,79	21,68	
	60		10,09		21,80	21,72	21,80	21,72	Compact
	12		1,98		21,81	21,76	21,81	21,76	
	75		2,02		21,81	21,76	21,80	21,76	
	93		1,91		21,80	21,73	21,80	21,73	
	62		10,08		21,82	21,77	21,81	21,77	Compact
	28		2,11		21,83	21,75	21,83	21,75	
	76		1,97		21,81	21,74	21,79	21,74	

Dimensional measurements

Irradiation test E 96-01

TABLE X

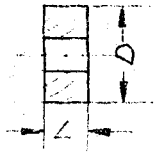

D means Diameter before irradiation in mm Accuracy ± 0,02
D' " " after " " " " ± 0,02
L means Length before irradiation in mm Accuracy +0,04 −0,02
L' " " after " " " " +0,04 −0,02

Company	Sample N°	Box N°	Length (mm)		diameter (mm)				Remarks
							Sample 90°turned		
			L	L'	D	D'	D	D'	
Dragon	3L4	IV	1,99		21,97	21,75	21,97	21,75	
	12L4		1,97		21,96	21,77	21,96	21,77	
	6G9		1,99		21,97	21,76	21,96	21,76	
	3G9		2,00		21,97	21,75	21,97	21,75	
	122-5		1,97		21,96	21,77	21,96	21,77	
	12E4		1,99		21,96	21,77	21,96	21,77	
	3E4		1,99		21,96	21,76	21,96	21,76	
	129-4		1,99		21,96	21,78	21,96	21,78	
	6C4		1,95		21,96	21,78	21,96	21,78	
	3C4		2,00		21,97	21,78	21,97	21,78	
	125-4		1,99		21,97	21,78	21,97	21,78	
	3A5		2,01		21,97	21,78	21,97	21,78	
	6A4		1,93		21,97	21,78	21,97	21,78	
	6A4C		13,75		21,97	21,80	21,97	21,80	Compact.

Dimensional measurements

Irradiation test E 96-01

TABLE XI

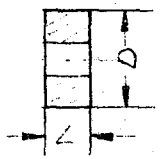

D means Diameter before irradiation in mm Accuracy ± 0,02
D' " " after " " " " ± 0,02
L means Length before irradiation in mm Accuracy +0,04 −0,02
L' " " after " " " " +0,04 −0,02

Company	Sample N°	Box N°	Length (mm)		diameter (mm)				Remarks
			L	L'	D	D'	Sample 90°turned D	Sample 90°turned D'	
K.F.A.	K56	IV	2,17		21,95	21,82	21,96	21,82	
	K57		1,96		21,95	21,82	21,96	21,82	
	K61		2,01		21,95	21,83	21,95	21,83	
	K62		2,06		21,95	21,84	21,96	21,84	
	K63		2,05		21,95	21,85	21,96	21,85	
	K65		1,95		21,95	21,84	21,96	21,84	
	K66		2,16		21,95	21,84	21,96	21,84	
	K69		2,03		21,95	21,85	21,96	21,85	
	K71		1,98		21,95	21,84	21,96	21,84	
	K72		1,90		21,95	21,83	21,96	21,83	
	K73		1,93		21,95	21,84	21,96	21,84	
	K74		2,01		21,96	21,85	21,95	21,85	

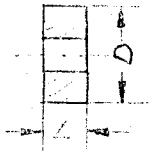

Dimensional measurements

Irradiation test E 96-01

TABLE XII

D means Diameter before irradiation in mm Accuracy ± 0,02
D' " " after " " " " ± 0,02
L means Length before irradiation in mm Accuracy +0,04 −0,02
L' " " after " " " " +0,04 −0,02

Company	Sample N°	Box N°	Length (mm)		diameter (mm)				Remarks
							Sample 90°turned		
			L	L'	D	D'	D	D'	
Bel.Nuc	C63	IV	10,07		21,83	21,77	21,83	21,77	Compact
	17		2,00		21,82	21,77	21,82	21,77	
	C47		10,13		21,82	21,77	21,83	21,77	Compact
	94		2,02		21,83	21,73	21,84	21,73	
	82		1,96		21,80	21,70	21,80	21,70	
	31		2,04		21,78	21,72	21,79	21,72	
	C50		10,13		21,81	21,74	21,82	21,74	Compact

TABLE XIII

Particle N°	$\Delta V/V_o$	Particle N°	$\Delta V/V_o$
1	14,8%	16	17,2%
2	22,0%	17	17,3%
3	8,7%	18	15,4%
4	21,5%	23	18,8%
7	7,0%	24	27,8%
8	15,1%	27	20,9%
14	19,7%	28	16,8%
15	19,4%	29	17,4%

NOTICE TO THE READER

All scientific and technical reports published by the Commission of the European Communities are announced in the monthly periodical **"euro-abstracts".** For subscription (1 year : B.Fr 1 025,—) or free specimen copies please write to .

Office for Official Publications
of the European Communities
Boîte postale 1003
Luxembourg
(Grand-Duchy of Luxembourg)

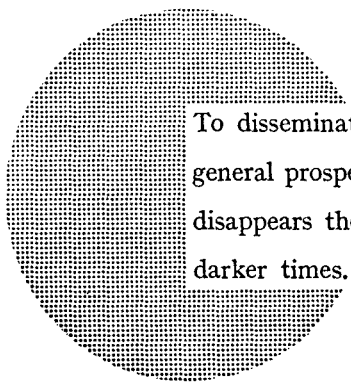

To disseminate knowledge is to disseminate prosperity — I mean general prosperity and not individual riches — and with prosperity disappears the greater part of the evil which is our heritage from darker times.

Alfred Nobel

SALES OFFICES

The Office for Official Publications sells all documents published by the Commission of the European Communities at the addresses listed below, at the price given on cover. When ordering, specify clearly the exact reference and the title of the document.

UNITED KINGDOM

H.M. Stationery Office
P.O. Box 569
London S.E. 1 — Tel. 01-928 69 77, ext. 365

BELGIUM

Moniteur belge — Belgisch Staatsblad
Rue de Louvain 40-42 — Leuvenseweg 40-42
1000 Bruxelles — 1000 Brussel — Tel. 512 00 26
CCP 50-80 — Postgiro 50-80

Agency :
Librairie européenne — Europese Boekhandel
Rue de la Loi 244 — Wetstraat 244
1040 Bruxelles — 1040 Brussel

DENMARK

J.H. Schultz — Boghandel
Møntergade 19
DK 1116 København K — Tel. 14 11 95

FRANCE

Service de vente en France des publications des Communautés européennes — Journal officiel
26, rue Desaix — 75 732 Paris - Cédex 15e
Tel. (1) 306 51 00 — CCP Paris 23-96

GERMANY (FR)

Verlag Bundesanzeiger
5 Köln 1 — Postfach 108 006
Tel. (0221) 21 03 48
Telex: Anzeiger Bonn 08 882 595
Postscheckkonto 834 00 Köln

GRAND DUCHY OF LUXEMBOURG

Office for Official Publications of the European Communities
Boîte postale 1003 — Luxembourg
Tel. 4 79 41 — CCP 191-90
Compte courant bancaire: BIL 8-109/6003/200

IRELAND

Stationery Office — The Controller
Beggar's Bush
Dublin 4 — Tel. 6 54 01

ITALY

Libreria dello Stato
Piazza G. Verdi 10
00198 Roma — Tel. (6) 85 08
CCP 1/2640

NETHERLANDS

Staatsdrukkerij- en uitgeverijbedrijf
Christoffel Plantijnstraat
's-Gravenhage — Tel. (070) 81 45 11
Postgiro 42 53 00

UNITED STATES OF AMERICA

European Community Information Service
2100 M Street, N.W.
Suite 707
Washington, D.C. 20 037 — Tel. 296 51 31

SWITZERLAND

Librairie Payot
6, rue Grenus
1211 Genève — Tel. 31 89 50
CCP 12-236 Genève

SWEDEN

Librairie C.E. Fritze
2, Fredsgatan
Stockholm 16
Post Giro 193, Bank Giro 73/4015

SPAIN

Libreria Mundi-Prensa
Castello 37
Madrid 1 — Tel. 275 51 31

OTHER COUNTRIES

Office for Official Publications of the European Communities
Boîte postale 1003 — Luxembourg
Tel. 4 79 41 — CCP 191-90
Compte courant bancaire: BIL 8-109/6003/300

OFFICE FOR OFFICIAL PUBLICATIONS OF THE EUROPEAN COMMUNITIES
Boîte postale 1003 — Luxembourg
6545